have developed a novel method for the immobilization of sulfated oligosaccharide onto a gold-coated SPR chip to prepare a "sugar chip" and devised an analytical system that can be applied to the binding interactions of a variety of structurally defined oligosaccharides in clustered structures that mimic nature.

In this paper, mono-, tri-, and tetravalent types of linker compounds containing one, three, or four aromatic amines and thioctic acid moieties were designed. The ligand moiety, a GlcNS6S-IdoA2S unit, was conjugated with these novel linker compounds to prepare a ligand conjugate using an optimized reductive amination reaction. The ligand conjugates were immobilized on a gold SPR sensor chip through an improved gold−sulfur (Au−S) permanent bond. By this approach, we were able to accurately measure the specific interactions of the GlcNS6S-IdoA2S structure in heparin with native human vWf protein and with the recombinant fragment of its A1 domain. To compare our method with conventional immobilization techniques, the GlcNS6S-IdoA2S unit was conjugated with a hydrophobic aromatic amine by a similar reductive amination reaction and immobilized through hydrophobic interactions with a hydrophobic 1-octanethiol-coated chip surface.

The goal of this current work was to refine the methods for immobilizing clustered oligosaccharides using these new techniques, to measure their uniformity and distribution on the SPR chip, and to measure the relative impact of ligand clustering on the binding of well-known heparin-binding proteins. Our long-term goal is to provide a simple, versatile, and reproducible method for studying glycosaminoglycan−protein interactions, which can be implemented by a wide range of investigators beyond the specialized laboratories that pioneered these approaches.

EXPERIMENTAL PROCEDURES

General Procedure. All reactions in organic media were carried out with freshly distilled solvents or with commercially available extra grade solvents purchased from Kanto Chem. Co. (Tokyo, Japan), Nacalai Tesque (Kyoto, Japan), or Wako Chem. Co. (Osaka, Japan). Silica gel column chromatography was performed using silica gel 60 (no. 9386, Merck & Co. Inc., Whitehouse Station, NJ). Spectral data were obtained as follows. Electrospray ionization time-of-flight mass (ESI-TOF/MS) spectra were obtained by Mariner (Applied Biosystems, Framingham, MA). ^{1}H NMR measurements were performed with JEOL (Tokyo, Japan) Lambda-500, GSX-400, and ECA-600. The chemical shifts are expressed in δ-values using tetramethylsilane (δ 0) or HDO (δ 4.65) as an internal standard.

SPR Experiments. SPR experiments were perfomed with SPR-670 (Nippon Laser and Electric Lab., Nagoya, Japan) under the recommended manufacture's guideline with a slight modification. Sensor chips used for SPR experiments were prepared as follows. The gold-coated chip was purchased from Nippon Laser and Electronics Lab. For ligand conjugates containing the thioctic acid moiety, the gold-coated chip was soaked in a 100 μM solution (methanol/water = 1/1, v/v) of the appropriate ligand conjugate at room temperature for 2 h or overnight, followed by subsequent washing with methanol/water containing 0.05% Tween-20, phosphate-buffered saline (PBS) at pH 7.4 containing 0.05% Tween-20, and PBS (pH 7.4). All washings were done with microwave irradiation for 5−30 min. The solvent for the binding experiment was PBS at pH 7.4 and run at a flow rate of 15 μL/min at 25 °C.

For ligand conjugates containing an octyl group, the gold chip was first soaked in 1 mM methanol solution of octanethiol at room temperature overnight, followed by washing with methanol, methanol/water (1/1, v/v), and PBS (pH 7.4) containing 10% 2-propanol. The octanethiol immobilized chip (self-assembled monolayer (SAM) chip) was set in the SPR-670; then the solution of ligand conjugate containing the octyl group in PBS (pH 7.4) containing 10% 2-propanol was loaded and run at a flow rate of 15 μL/min at 25 °C. The ligand conjugate became immobilized through a hydrophobic interaction between the SAM on the chip and the octyl group of the conjugate. This was monitored by SPR-670. The subsequent saccharide−protein binding experiments were done using PBS (pH 7.4) containing 10% 2-propanol. Bovine serum albumin (BSA) was employed as the control, nonspecific protein of study. It is ubiquitous in biological systems and is known to have low nonspecific interactions with sulfated polysaccharides.

Synthesis of Compounds. Details of compound syntheses can be found in Supporting Information.

RESULTS

Preparation of Oligosaccharide-Linker Conjugates (Abbreviated as "Ligand Conjugates"). Mono-, tri-, and tetravalent linker molecules and ligand conjugates were prepared as illustrated in Schemes 1−5. The linker compounds possessed one, three, or four incorporating points, and the ligand conjugates were composed of the linker attached to a structurally defined, biologically active sulfated disaccharide unit (GlcNS6S-IdoA2S) or D-glucose as a control. All the structures of the compounds were confirmed by ESI-TOF/MS and NMR.

Monovalent Linkers and Ligand Conjugates (Schemes 1 and 2). The reaction of *m*-phenylenediamine **1** with di-*t*-butyl dicarbonate in methanol solution yielded 3-(*t*-butoxycarbonylamino)phenylamine **2**. The compound **2** was then reacted with thioctic acid **3** in dichloromethane to give the thioctamide derivative **4**, followed by treatment with trifluoroacetic acid to yield the linker compound **5**. A reductive amination reaction with a sulfated trisaccharide **6** (synthesized as previously reported (*18*)) was employed to incorporate the disaccharide unit into a novel ligand conjugate **7** (Mono-GlcNS6S-IdoA2S-Glc). By a similar reductive amination reaction using D-glucose, a control ligand conjugate **8** (Mono-Glc) was also prepared.

For the hydrophobic immobilization strategy (Scheme 2), a hydrophobized ligand conjugate **13** containing the GlcNS6S-IdoA2S unit was prepared. The reaction of 4-aminobenzoic acid **9** with di-*t*-butyl dicarbonate in methanol solution yielded 4-(*t*-butoxycarbonylamino)benzoic acid **10**. Further reaction with *n*-octylamine in dichloromethane gave benzamide **11**, which was then treated with trifluoroacetic acid to yield the hydrophobic linker *N*-octyl-4-aminobenzamide **12**. The linker **12** was coupled with the trisaccharide **6** using a reductive amination reaction to give the hydrophobized compound **13** (Hydro-mono-GlcNS6S-IdoA2S-Glc). A similar reductive amination was performed with D-maltose to give D-glucopyranoside-containing ligand conjugate **14** (Hydro-mono-Glc-Glc), which was used for the control experiments.

Trivalent Linker and Ligand Conjugate (Scheme 3). For the trivalent type linker compound **24**, the Michael addition reaction followed by reduction with Raney nickel was applied to nitromethane **15** to give tribranching amine **18** according to Weis and Newkome (*19*) with a slight modification. The production of a side product, di-*t*-butyl 4-[(2-*t*-butoxycarbonyl)ethyl]-4-aminoheptanedicarboxylate, was less than 5% in this case. To the amine moiety **18**, a *Z*-glycine unit was incorporated, which served as a spacer between the branching part and the further incorporating thioctic acid moiety. The coupling reductive amination reaction was performed as above with a slight modification, in which dimethylacetoamide was used to dissolve the tribranched linker compound **24** instead of methanol. The reaction was monitored with thin-layer chromatography (TLC) and ESI-TOF/MS. After confirmation of the formation of the Shiff base, the ratio of the mixed solvent was changed to promote a more efficient reduction reaction. We found that it

Scheme 1. Synthesis of Monovalent Linker and Ligand Conjugates

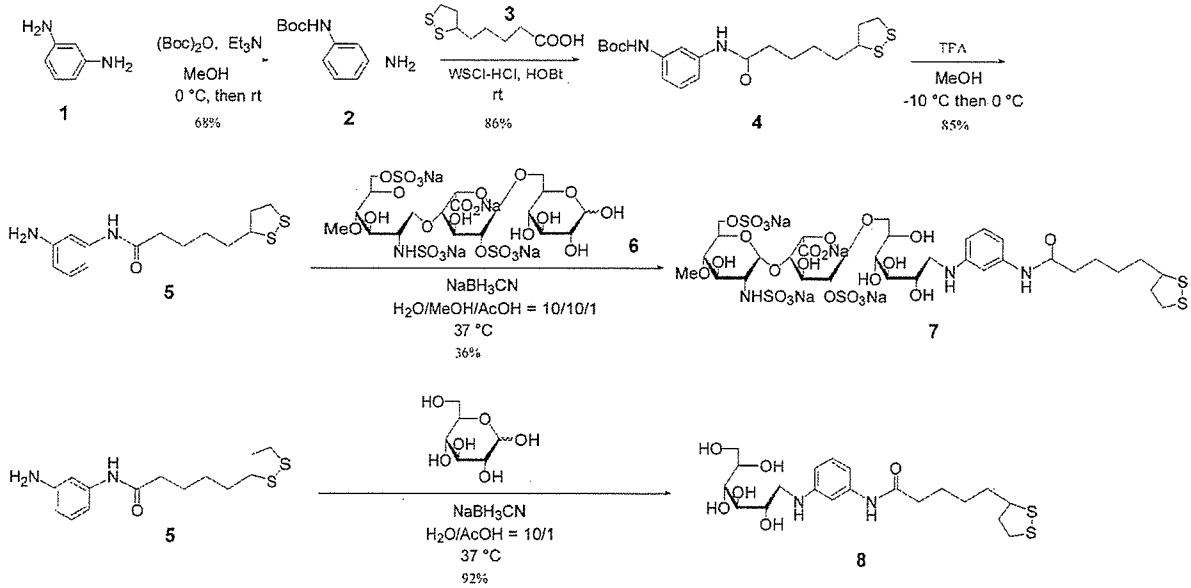

Scheme 2. Synthesis of Hydrophobized Monovalent Linker and Ligand

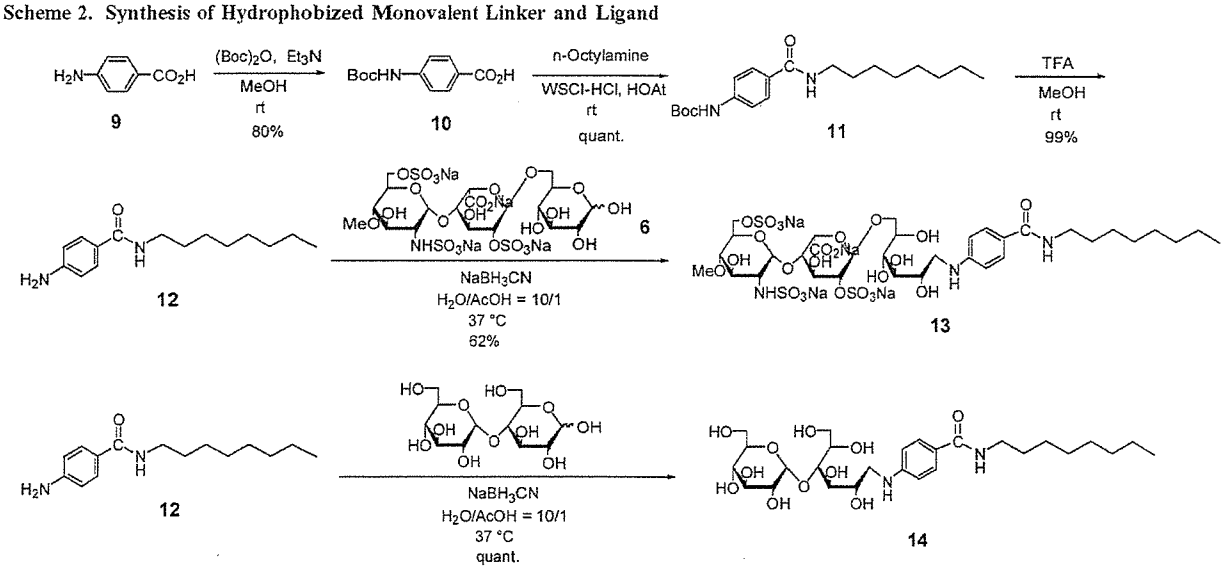

was important to maintain the pH of the solvent between 3 and 4 to increase the conversion of the reaction. A 5-fold ratio of sulfated trisaccharide **6** to the linker **24** was necessary to incorporate all three of the aromatic amine moieties in **24** to produce **25** (Tri-GlcNS6S-IdoA2S-Glc). The lower than expected yield (66%) was due to losses during purification.

Tetravalent Linker and Ligand Conjugate (Scheme 4). The tetravalent linker compound **34** was prepared according to Ashton et al. (*20*) with modifications. In brief, two units of aminobenzoic acid moieties were incorporated into the two primary amines in diethylenetriamine with a relatively good yield by precisely controlling their molar ratio. For the spacer between the thioctic acid moiety and the branching part, *Z*-glycine was incorporated to give compound **30**. The condensation of **27** and **31** needed a stronger condensation reagent, pentafluorophenyl diphenylphosphinate (FDDP), to give the tetravalent linker unit containing four units of aromatic amine derivative **35**. The incorporation of sulfated disaccharide units to yield **35** was performed by similar reaction conditions as applied to **24**. A 5-fold ratio of sulfated trisaccharide **6** to the linker **35** was also necessary to incorporate all four of the aromatic amine moieties in **35** to produce **36** (Tetra-GlcNS6S-IdoA2S-Glc-short). Diminished yield (40%) was again due to losses during purification.

Tetravalent Linker and Ligand Conjugate with Longer Spacer Arm (Scheme 5). In order to create an immobilized oligosaccharide cluster with a longer leash, or spacer arm, we created tetravalent linker **48** and ligand conjugate **49** by modifying **35** and **36**, respectively (Scheme 5). An oligo(ethylene glycol) unit was incorporated between the branched part and the thioctic acid moiety. The oligo(ethylene glycol) unit was derivatized according to Houseman and Mrksich (*6*) to afford the *O*-toluenesulfonyl compound **40**. By the S_N2 reaction with sodium azide, an azide unit was incorporated. After hydrolysis, we obtained **42**, which was then used for the spacer unit instead of *Z*-glycine in the preparation of **30**. The azide moiety was converted to amine by mild reduction, and the thioctic acid moiety was condensed to the amino group, followed by deblocking of the aromatic amine by trifluroacetic acid to yield the tetravalent linker **48** containing an oligo(ethylene glycol)

Scheme 3. Synthesis of Trivalent Linker and Ligand Conjugate

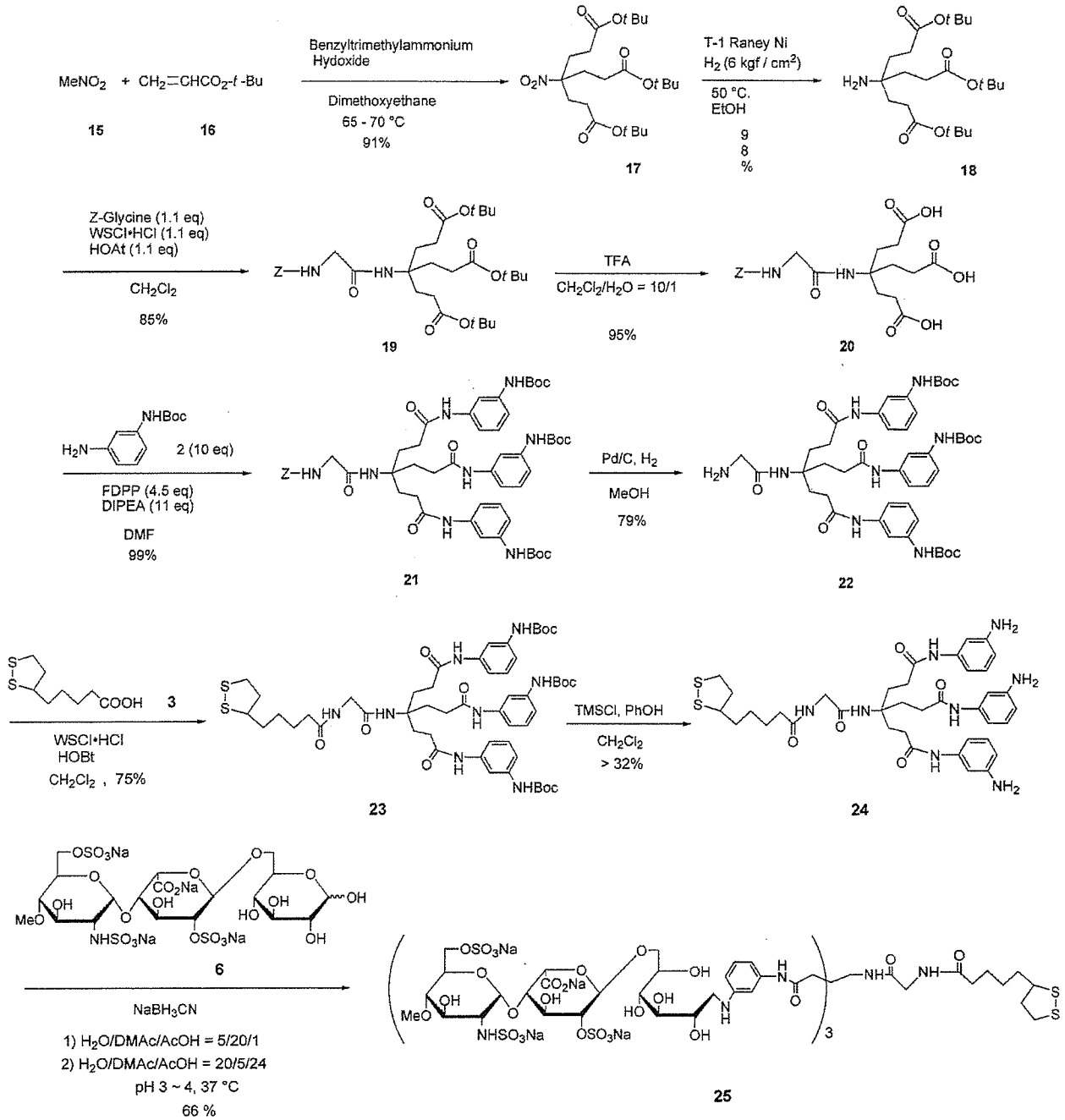

unit. The incorporation of sulfated disaccharide units into **48** was performed by the same reaction as applied to **25**. A 7-fold ratio of sulfated trisaccharide **6** to the linker **48** was necessary to incorporate the four aromatic amine moieties in **48** to prepare **49** (Tetra-GlcNS6S-IdoA2S-Glc-long). Yield (22%) was again diminished primarily due to purification. All the structures of the compounds were confirmed by ESI-TOF/MS and ^{1}H NMR.

Comparison of Immobilization Methods. The monovalent ligand conjugates **7** (Mono-GlcNS6S-IdoA2S-Glc) and **8** (Mono-Glc) were first immobilized on the gold chip by soaking the chip in the 100 μM 50% aqueous methanol solution of the ligand conjugate for 2 h or overnight at room temperature with gentle agitation. It was predicted that the ligand conjugates would be immobilized on the gold-coated chip through direct Au−S bonding. With use of an SPR670 apparatus (Nippon Laser and Electronics Lab, Nagoya, Japan), a binding interaction to the ligand moiety on the chip was confirmed when 2 μM of the synthetic peptide KDRKRSELRRIASQVK (a discrete heparin-binding domain of human vWf (*21*), abbreviated as vWf-peptide) was injected over the surface of the chip in the apparatus (Figure 1a). Because minimal binding was observed with 1.5 μM of BSA, it was not even necessary to subtract a nonspecific binding value.

When the control Mono-Glc was immobilized using the same method, no significant increase in resonance units was observed even though a high concentration of synthetic vWf-peptide was used (Figure 1b). In contrast, a typically positive binding saturation curve was seen with the Mono-GlcNS6S-IdoA2S-

Scheme 4. Synthesis of Tetravalent Linker Containing Short Spacer Arm and Ligand Conjugate

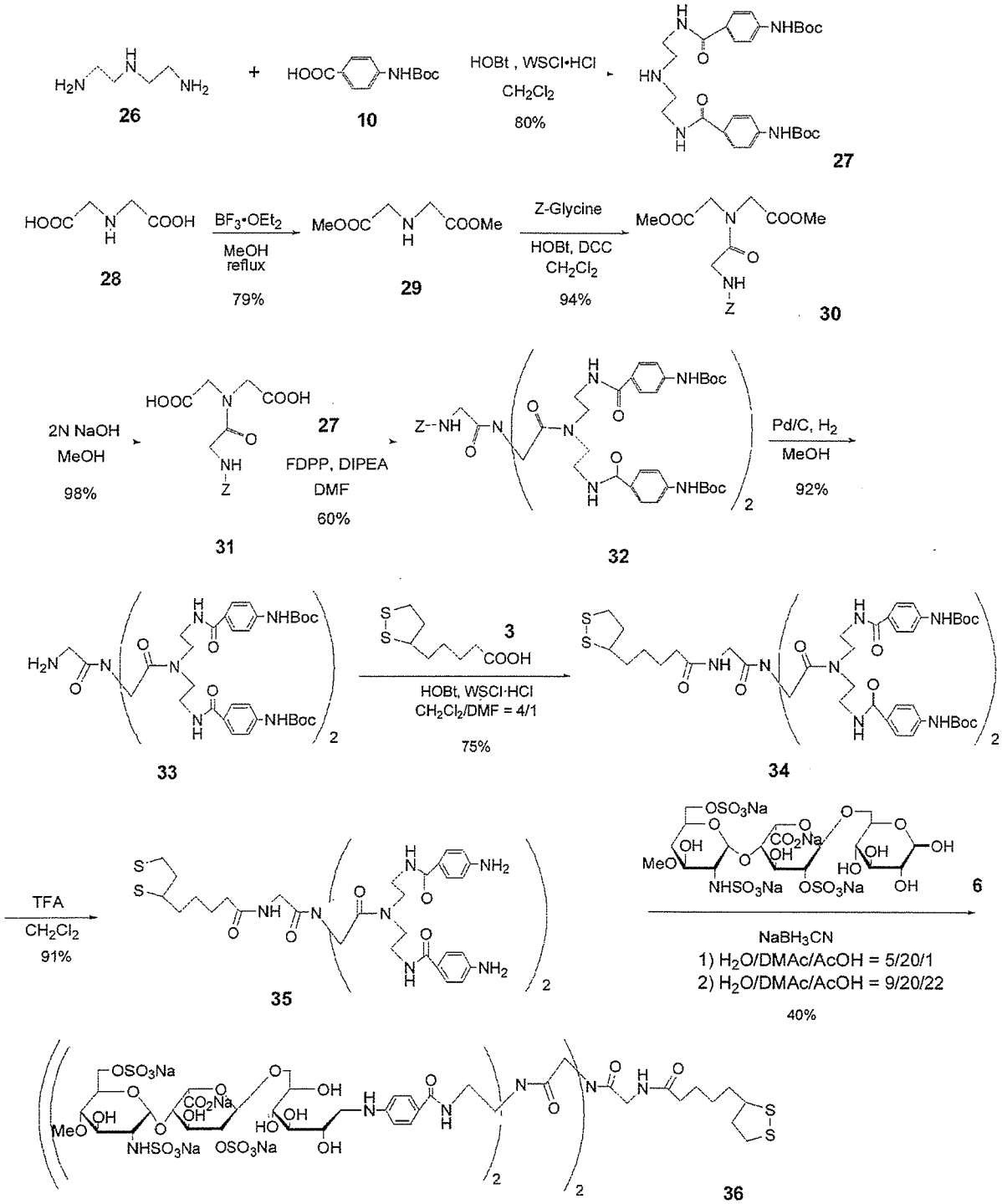

Glc immobilized chip. The K_D, dissociation constant, was estimated to be 220 nM, very close to that reported previously (370 ± 100 nM) for unfractionated heparin and vWf using a conventional radioligand binding assay (*21*).

This direct, covalent immobilization method was then compared to a conventional hydrophobic method of immobilization. A self-assembled monolayer (SAM) of octanethiol was first prepared on the chip as previously reported (*10*, *11*). The SAM chip was set in the SPR670 apparatus and a solution of **13** or **14** was loaded on the chip in phosphate-buffered saline. The total amount of **13** or **14** that was immobilized on the sensor chip is indicated by the differences in resonance units (ΔRU^1) at equilibrium shown in Figure 2a. Then, the binding of synthetic vWf-peptide was evaluated. Figure 2b shows that the vWf-peptide bound to both the sulfated oligosaccharide SAM chip (using **13**, Hydro-mono-GlcNS6S-IdoA2S-Glc) and the control SAM chip (using **14**, Hydro-mono-Glc-Glc). These nonspecific interactions were confirmed when BSA was tested on the same SAM sensor chip; strong binding of BSA to both chips was observed (data not shown).

Scheme 5. Synthesis of Tetravalent Linker Containing Long Spacer Arm and Ligand Conjugate

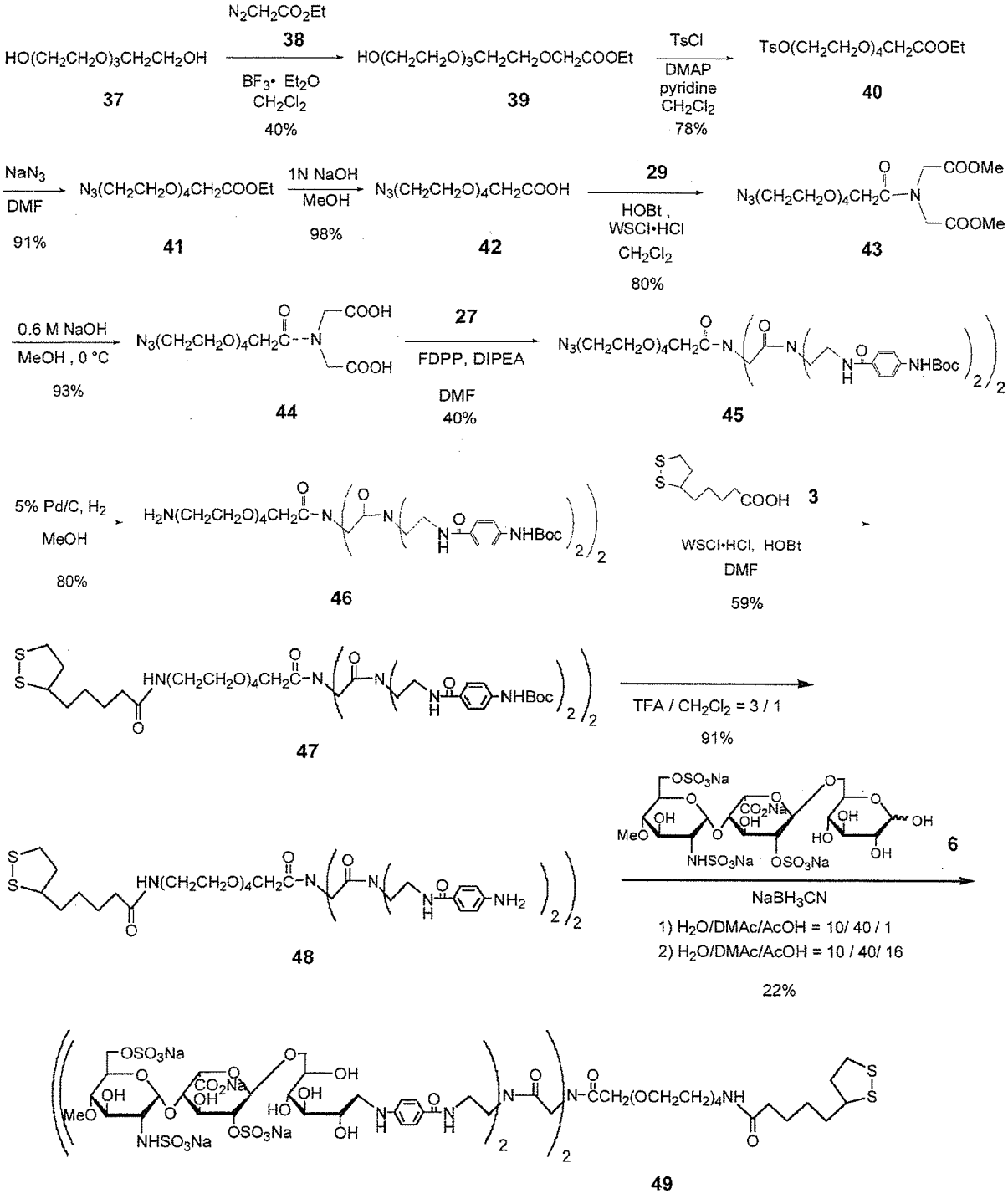

Evaluation of Immobilization of the Ligand Conjugates via the Covalent Attachment Method. The tri- and tetravalent ligand conjugates containing the sulfated disaccharide units were immobilized on gold chips as described above, and nonspecific binding to 1.5 μM BSA was measured. Experience showed that the chips prepared in this manner were quite stable, retaining full binding potency when stored dry at room temperature for 6 months (data not shown). Figure 3 shows that chips immobilized with conjugates **25** (Tri-GlcNS6S-IdoA2S-Glc) and **49** (Tetra-GlcNS6S-IdoA2S-Glc-long) showed very little nonspecific binding, just as was observed in Figure 1a with the Mono-GlcNS6S-IdoA2S-Glc (conjugate **7**). The tetravalent conjugate with the short linker arm (conjugate **36**) exhibited high nonspecific binding (Figure 3) that is typical of a BSA interaction with a bare, unmodified gold chip. Hence, we concluded that conjugate **36** did not achieve optimal immobilization to the gold chip. Its more flexible linkage chemistry, combined with a short spacer arm, may have obscured the accessibility of the S−S portion of the linker for effective immobilization. In subsequent experiments, trivalent

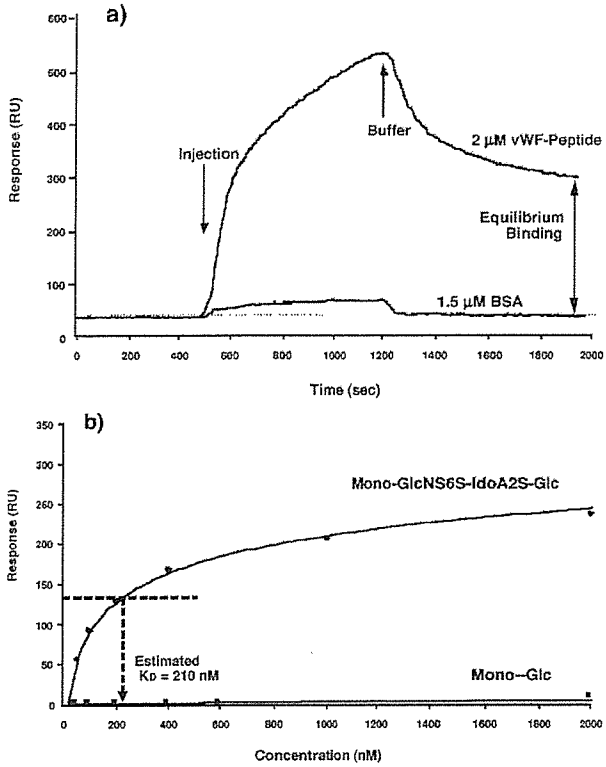

Figure 1. (a) Binding of vWf-peptide and BSA to Mono-GlcNS6S-IdoA2S-Glc (ligand conjugate **7**) on the chip was observed (flow rate = 5 μL/min, temp = 25 °C, pH 7.4, PBS); (b) the equilibrium binding data were used to generate a saturation curve for vWf-peptide binding to Mono-GlcNS6S-IdoA2S-Glc and to the control ligand conjugate **8** (Mono-Glc).

ligand conjugate **25** (Tri-GlcNS6S-IdoA2S-Glc) and ligand conjugate **49** (Tetra-GlcNS6S-IdoA2S-Glc-long) were used in addition to Mono-GlcNS6S-IdoA2S-Glc (compound **7**).

Density and Homogeneity of Immobilization. We wished to determine how the density of immobilization of different conjugates on the chip would influence binding activity. Accordingly, different percentages of biologically active ligand conjugates were individually diluted with the control glucose monovalent conjugate **8** (Mono-Glc) and immobilized as above. The relative concentration of the immobilized sulfated disaccharide was determined by attenuated total reflection (ATR) FT-IR spectra with IRPrestige-21 equipped with MIRacle (Shimdzu Co., Kyoto, Japan). Figure 4a shows parts of the ATR-FT-IR spectra for the region of sulfate groups (1200 and 1303 cm^{-1}) on the gold surface, where Mono-GlcNS6S-IdoA2S-Glc was immobilized over a range of relative densities. The intensity of absorbance increased as the chip was coated with an increasing percentage of Mono-GlcNS6S-IdoA2S-Glc in the ligand conjugate mixture. The absorbance between 1200 and 1303 cm^{-1} was integrated and plotted against the relative concentration of ligand conjugate including the sulfated disaccharide units. As shown in Figure 4b–d, there were linear relationships between the integral of absorbance for sulfate groups on the chip and the relative concentration of the active ligand conjugate in the mixture, suggesting that the sulfated disaccharide units were homogeneously immobilized on the gold surface. In other words, the relative density of ligand oligosaccharides on the chip surface can be controlled by admixing the Mono-Glc ligand conjugate, since the efficiency of S–Au bonding does not appear to be altered between Mono-GlcNS6S-IdoA2S-Glc and Mono-Glc.

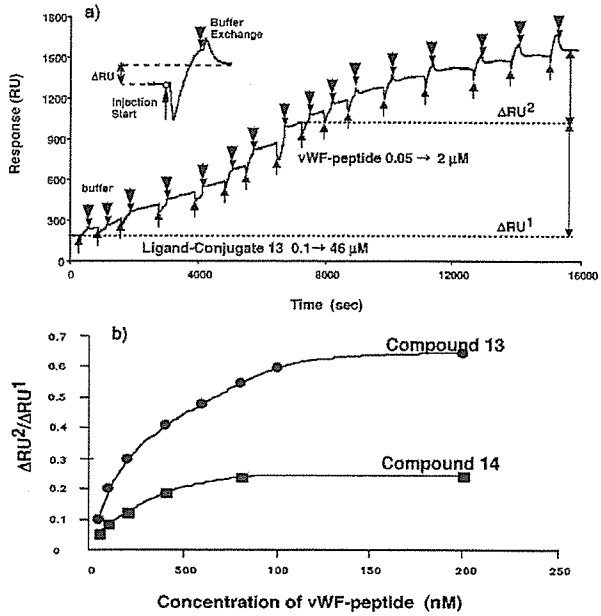

Figure 2. (a) Immobilization of ligand conjugate **13** (Hydro-mono-GlcNS6S-IdoA2S-Glc) containing GlcNS6S-IdoA2S on the SAM chip and the binding of vWf-peptide were observed (flow rate = 15 μL/min, temp = 25 °C, pH 7.4, PBS containing 10% 2-propanol); (b) the equilibrium binding data were used to generate saturation curves for the binding of vWf-peptide to the ligand conjugate **13** and to the control **14** (Hydro-mono-Glc-Glc).

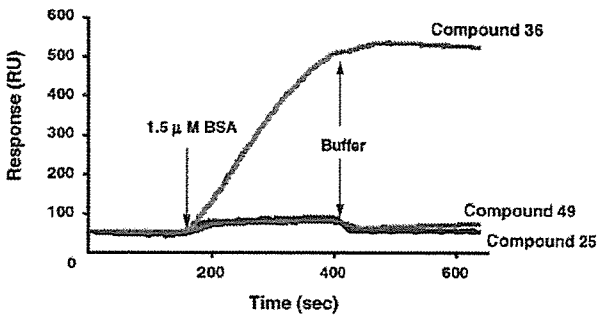

Figure 3. Binding of BSA to the sulfated disaccharide, GlcNS6S-IdoA2S, immobilized chips by ligand conjugates **25** (Tri-GlcNS6S-IdoA2S-Glc), **36** (Tetra-GlcNS6S-IdoA2S-Glc-short), and **49** (Tetra-GlcNS6S-IdoA2S-Glc-long). The immobilization and SPR experiment were done as described in the Experimental Procedures.

Measurement of Binding Affinities for Model Heparin-Binding Proteins. To evaluate the influence of oligosaccharide immobilization density on protein binding, 2 μM vWf-peptide was injected over chips immobilized with different percentages of Mono-GlcNS6S-IdoA2S-Glc to Mono-Glc immobilized chip (Figure 5). The binding affinity decreased as the relative density of the surface-immobilized sulfated disaccharide units diminished. When the biologically active disaccharide comprised less than 40% of the immobilized ligand, binding was minimal.

We also studied the binding of the recombinant human vWf-A1 domain (rhvWf-A1) (*22*). This protein contains the same heparin-binding domain studied in Figure 5 (vWf-peptide) but also includes a secondary or cooperative heparin binding site (*23*). The three ligand conjugates, Mono-GlcNS6S-IdoA2S-Glc, Tri-GlcNS6S-IdoA2S-Glc, and Tetra-GlcNS6S-IdoA2S-Glc-long, were immobilized at 100% and 50% density (mixed 1:1 with Mono-Glc). Table 1 compares the effects of clustering (valency) and immobilization density on the binding parameters

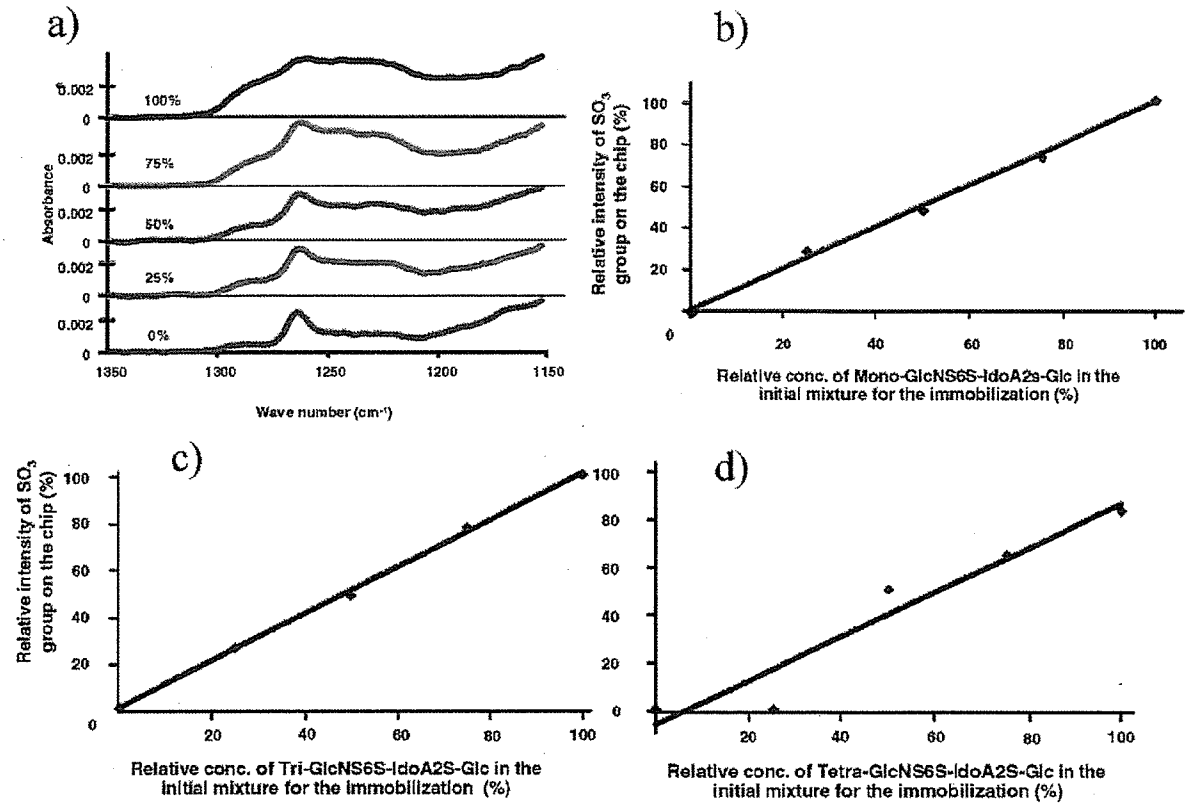

Figure 4. (a) ATR-FT-IR spectra of Mono-GlcNS6S-IdoA2S-Glc immobilized chip. The immobilization was done by adding Mono-GlcNS6S-IdoA2S-Glc to the control ligand conjugate (Mono-Glc) with changing concentration (0 to 100%). Intensity of ATR-FT-IR was plotted against the initial concentration of (b) Mono-GlcNS6S-IdoA2S-Glc (R^2 = 0.9984), (c) Tri-GlcNS6S-IdoA2S-Glc (compound **25**; R^2 = 0.9993), and (d) Tetra-GlcNS6S-IdoA2S-Glc-long (compound **49**; R^2 = 0.9610) in the ligand conjugate mixture.

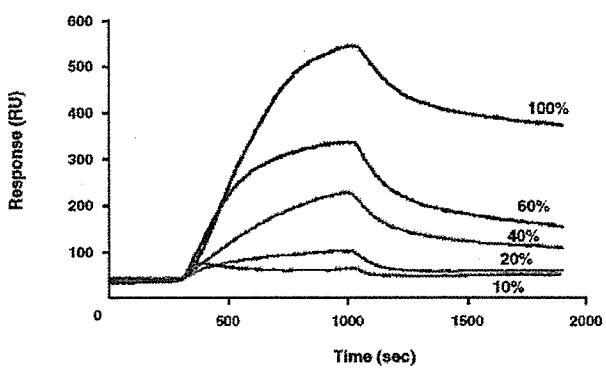

Figure 5. SPR sensorgram of vWf-peptide binding. Chips were immobilized with increasing proportions of Mono-GlcNS6S-IdoA2S-Glc, with the total concentration ([Mono-GlcNS6S-IdoA2S-Glc] + [Mono-Glc]) fixed at 100 μM. vWf-peptide was 2 μM.

(calculated from kinetic data using the analytical software of the SPR670).

The increased clustering of oligosaccharides provided by the tri- and tetravalent conjugates uniformly yielded lower dissociation constants K_D and lower dissociation rates k_d. The monovalent conjugate had an ~2.5−3-fold higher K_D and k_d. A 50% decrease in the density of immobilization hardly changed the binding parameters of the tri- and tetravalent ligand conjugates, while the same decrease in density of the monovalent ligand raised the K_D by 1.5-fold and doubled the k_d.

We then measured oligosaccharide binding of an even more complex version of this heparin-binding protein, the whole human vWf protein. A single vWf monomer protein is 270 kDa

Table 1. Binding of rhvWf-A1: Clustering Effect of Sulfated Oligosaccharide on the Chip

ligand conjugates	ratio	K_D [a] (μM)	k_a [b] ($M^{-1}\,s^{-1} \times 10^3$)	k_d [c] ($s^{-1} \times 10^{-3}$)
Mono-GlcNS6S-IdoA2S-Glc	100/0	2.60	8.38	21.9
Mono-GlcNS6S-IdoA2S-Glc/ Mono-Glc	50/50	3.79	14.6	55.2
Tri-GlcNS6S-IdoA2S-Glc	100/0	1.20	6.60	8.05
Tri-GlcNS6S-IdoA2S-Glc/ Mono-Glc	50/50	1.50	4.52	6.83
Tetra-GlcNS6S-IdoA2S-Glc	100/0	0.99	6.50	6.44
Tetra-GlcNS6S-IdoA2S-Glc/ Mono-Glc	50/50	1.00	5.24	5.26

[a] k_d/k_a (dissociation constant). [b] Association rate. [c] Dissociation rate.

Table 2. Binding of Whole rhvWf: Lack of Clustering Effect of Sulfated Oligosaccharide on the Chip

ligand conjugates	ratio	estimated K_D (nM)
Mono-GlcNS6S-IdoA2A-Glc	100/0	35
Mono-GlcNS6S-IdoA2A-Glc/Mono-Glc	20/80	41
Tri-GlcNS6S-IdoA2A-Glc	100/0	24
Tri-GlcNS6S-IdoA2A-Glc/Mono-Glc	20/80	27
Tetra-GlcNS6S-IdoA2A-Glc	100/0	35
Tetra-GlcNS6S-IdoA2A-Glc/Mono-Glc	20/80	32

molecular mass, but it forms large multimers reaching several million daltons, displaying multiple heparin-binding sites. Experiments were performed using mono-, tri-, and tetravalent (long) ligand conjugates immobilized at 100% and 20% relative concentrations. Table 2 summarizes the estimated binding constants derived from the data illustrated in Figure 6a−c. The estimated K_D values were all very similar and did not depend

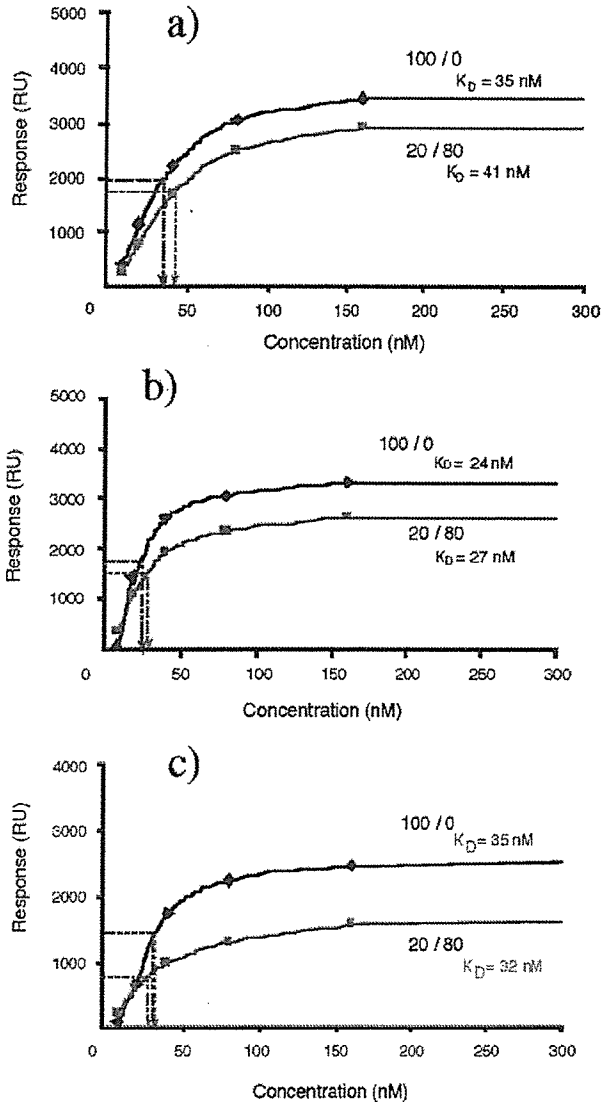

Figure 6. Equilibrium binding of whole hvWf protein to chips immobilized with Mono-GlcNS6S-IdoA2S-Glc/Mono-Glc (a), Tri-GlcNS6S-IdoA2S-Glc/Mono-Glc (b), and Tetra-GlcNS6S-IdoA2S-Glc-long/Mono-Glc (c). The ratios of Mono-GlcNS6S-IdoA2S-Glc, Tri-GlcNS6S-IdoA2S-Glc, or Tetra-GlcNS6S-IdoA2S-Glc-long/Mono-Glc were 100/0 and 20/80.

on the relative density of the immobilization of the ligand conjugates nor the multivalency of the ligand conjugate.

Finally, we studied the binding affinity for a completely different heparin-binding protein, human basic fibroblast growth factor (bFGF). Here we performed competitive binding studies with immobilized Tri-GlcNS6S-IdoA2S-Glc (compound **25**) and bFGF (200 nM) in solution phase admixed with increasing concentrations of unfractionated pharmaceutical grade heparin (Nacalai Tesque, from porcine intestine, average MW = 15000). Figure 7a shows that with increasing concentrations of soluble heparin, the binding of 200 nM of bFGF decreased. Figure 7b shows the estimated IC_{50} of heparin to be 50−100 nM, which is close to the reported K_D of bFGF for heparan sulfate proteoglycan (*24*).

DISCUSSION

The first goal of this work was to devise and refine a simpler and nondestructive strategy for immobilizing structurally defined

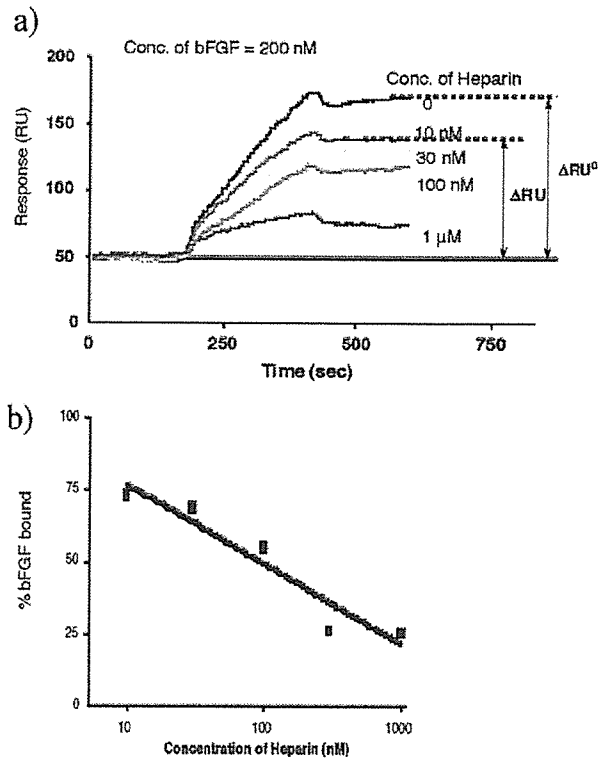

Figure 7. (a) SPR sensorgram of competitive heparin binding to bFGF. Mixtures of bFGF (200 nM) with or without soluble commercial heparin (Nacalai Tesque, from porcine intestine, average MW = 15000) were run on the chip of Tri-GlcNS6S-IdoA2S-Glc. (b) Relationship between the concentration of heparin and ΔRU at equilibrium.

oligosaccharides on a chip for SPR. When ligand immobilization methods were compared, the direct, covalent immobilization to the gold surface via Au−S bonds yielded minimal nonspecific binding interactions, as examplified by the negligible binding of BSA, and minimal protein binding to the control glucose ligand. In contrast, BSA bound to the self-assembled monolayer of octanethiol through nonspecific hydrophobic interactions, and the vWf-peptide bound with some measurable affinity even to the negative control glucose ligand.

We also sought to develop a linkage method that was simple, nondestructive, and applicable to a wider range of naturally occurring oligosaccharides. The reductive amination coupling to linker compounds containing aromatic amines offered more precise, quantitative control over the linkage process, especially when compared with techniques of mass immobilization using the lysine groups of albumin or other proteins. The reductive amination reaction is certainly a well-established method. It is typically used for the labeling of oligosaccharides, such as in the pyridyl amination reaction. In that case, excess amounts of pyridylamine are used, and the labeled compounds have been used primarily for the analysis of the structure of oligosaccharides. With use of this known pyridyl amination reaction, ligand conjugates for the immobilization of oligosaccharides onto the gold surface cannot be obtained.

Other methods have used the amino groups in a carrier protein, like bovine serum albumin, to form multivalent ligand oligosaccharides with dramatic increases in binding affinity. We previously examined the reductive amination strategy in detail and found the optimized conditions (*25*). In brief, the reaction should be done at around pH 4 to get a high yield. Therefore, regular alkyl amines gave lower yields because of the protonation of the amino group. If the pH is increased to over seven to have more free amino groups, the simple reduction at the

reducing end of oligosaccharide predominated. Thus, we found that aromatic amines had the optimal properties. Using those linker compounds described here, many other oligo- and polysaccharides including sialic containing ones, unfractionated high molecular weight heparin, low molecular weight heparins (LMWHs) prepared by several different methods, or amyloses, were also successfully conjugated. Those results will be reported soon.

Gold−sulfur immobilization schemes have also been used by Ratner et al. (*26*) and Horan et al. (*5*), but the regular thiol-containing compounds they used for self-assembling monolayers can form both S−S and S−H bonds, depending on the concentration. Therefore, purification of these oligosaccharide−thiol conjugates may be challenging, with low yields. Our current approach using a linker compound containing a thioctic acid with intramolecular S−S bonds avoids these significant challenges in purification during the synthesis. The advantages of using thioctic acid have been recognized in our patent (*27*) and in a recent publication (*28*).

The second purpose was to precisely quantify the nanostructural contributions of clustering, or valency, on the affinity of oligosaccharide ligands for increasingly complex heparin-binding proteins by varying spacer-arm length, immobilization density, and valency. Here, the distinction should be made between the minimal oligosaccharide binding unit and the minimal functional oligosaccharide necessary for biological activity. Often, a di- or trisaccharide of specific structure can be identified as the key binding unit (as we have done previously (*17*)). However, an isolated disaccharide often has low affinity and biological activity for the target protein. When multiple copies of this minimal binding unit are spaced appropriately (either within a single heparin chain or by adjacent chains), then the ligand protein may engage in higher affinity equilibrium binding that results in biological effects. Thus, overall the tri- or tetravalent compounds had higher affinities than the monovalent type, and the affinity was less dependent on their relative density on the surface of the SPR gold chip (Table 1). That is, when multivalency was incorporated as an intrinsic property of the ligand, variations in the density of immobilization had significantly less effect on the observed affinities. In contrast, the affinities of the monovalent ligand conjugates dropped dramatically when their relative density fell to 50%. Even though the changes shown in Table 1 were small, we observed a larger increase of K_D (lower affinity) of rhvWf-A1 when the relative density was decreased to 20% (data not shown). A larger k_d rate constant (Table 1) was observed compared to 100% density, suggesting that the observed binding of rhvWf-A1 occurred via equilibrium binding. These results support the concept that oligosaccharide ligand valency and density are important determinants for protein affinity. In biological systems, the key minimal oligosaccharide structure may either be spaced appropriately as a repeating unit within the same polymer chain or be displayed by clusters of neighboring polymers.

In addition to intrinsic ligand valency and density, it was interesting to find that a third factor also influenced equilibrium binding, the complexity of the heparin-binding protein. In the case of the simplest monovalent disaccharide ligand conjugate, its binding to a single, linear heparin-binding domain peptide (vWf-peptide) was highly dependent on the density of immobilized ligand (Figure 5). The monovalent ligand's interaction with a more complex heparin-binding protein (rhvWf-A1 containing major and minor heparin-binding domains) was still dependent on immobilization density, but slightly less so (Table 1). Finally, the monovalent ligand's interaction with the native multimeric vWf protein (containing multiple heparin-binding sites) showed the least dependency on immobilization density (Table 2). The binding of multivalent oligosaccharide ligands to increasingly complex heparin-binding proteins was much less sensitive to immobilization density. The trivalent and tetravalent constructs with the long spacer arm exhibited no significant change in K_D with reduced density.

Microarrays of synthetic heparin oligosaccharides have been reported very recently (*29*). But from these "sugar chips", the influence of the heparin-binding protein lends insights into the nature of protein−glycosaminoglycan binding mechanisms. It suggests that as the protein presents a multiplicity of heparin-binding sites, the interactions with the sulfated disaccharide units change from static multipoint binding to kinetic equilibrium binding. Neither ligand clustering nor density seemed to play as important a role in binding native multimeric hvWf, most likely because of the many widely spaced ligand binding sites presented by the protein itself. These results point to one unexpected advantage of this current technology: by altering the relative density and valency of the ligand on the surface, one can easily distinguish between single-site and multisite binding interactions between proteins and oligosaccharides. Thus, the heparin-binding properties of an unknown protein can be deduced.

Another utility of this approach is illustrated by the competitive binding assay using the trivalent ligand conjugate and human bFGF. We measured similar competition curves by soluble heparin against the monovalent or tetravalent ligand conjugates (data not shown). This technique can be easily applied, for example, to the screening of inhibitors or competitors of growth factors.

In previous work, we have found that the surface of the commercial gold-coated chip, at nanometer scale, is not perfectly flat. It varies in vertical elevation by as much as 10 nm up and down (detected by atomic force microscopy (AFM), data not shown). Thus, it was not surprising that the immobilization of ligands less than 2 nm in size might be affected by surface conditions, producing less consistent two-dimensional clustering of ligand on the surface. However, in the tri- or tetravalent type ligand conjugates, the biologically active oligosaccharides were dispersed within 2−3 nm, making a nanometer-sized cluster, which is independent of the surface irregularities of the gold-coated chip. Up to a point, a clustering-type effect can be achieved by immobilizing monovalent ligands at a higher density, but the nanostructural properties of the surface may interfere with the consistency and reproducibility of this effect. One explanation may be that the multivalent linkers are less affected by these surface conditions and thus show comparable affinities at lower density. Among them, the trivalent type may have some advantages. The trivalent linker contains an sp^3 carbon at the branching point. This branching makes a rigid structure and therefore gives an open space for the thioctic acid moiety (intramolecular S−S part) to immobilize the ligand conjugate to the gold surface. In contrast, the tetravalent type linker's branching parts are flexible enough to allow the large oligosaccharides to move apart and potentially mask the thioctic acid moiety. The ligand conjugate **36** (short spacer, tetravalent) was not able to be effectively immobilized. When a longer spacer arm was inserted (four units of ethylene glycol between the branching part and the thioctic acid moiety), compound **49** could then be successfully immobilized.

CONCLUSION

We have studied the binding of mono- and multivalent oligosaccharide ligands to increasingly complex heparin-binding protein structures. We have devised relatively simple and novel nondestructive methods of conjugation and immobilization that are applicable to a wide range of synthetic or naturally occurring oligosaccharides. The data show that clustering of the biologically active oligosaccharides enhances their affinity for simple

heparin-binding motifs and reduces the impact of surface irregularities or variations in the density of immobilization. For more complex heparin-binding proteins, the density of immobilization and the degree of ligand valency play less of a role. This relative dependence on density can thus be used as one rapid method to characterize the nature of the glycosaminoglycan−protein interaction.

Several technical advantages are conferred by these approaches. The reductive amination technique using an aromatic amino moiety offers a simpler, more quantitatively precise method of conjugation than that reported by Feizi and Chai (*30*). It is suitable for any oligosaccharide with a reducing end and does not require significant modification of their functional sulfate groups. The sulfur−gold immobilization using a thioctic acid moiety permits tighter control of the sulfur reactions, and easier purification of the conjugate. With tri- or tetravalent linkers, the oligosaccharides can easily be incorporated as a clustered form that mimics nature. These novel applications of SPR offer the potential to elucidate a range of fundamental structure−function relations of oligosaccharide−protein interactions at the molecular level and hold promise as a novel approach to rapid throughput screening of new bioactive molecules..

ACKNOWLEDGMENT

We wish to thank Mr. Y. Murakami (Shimazu Co., Kyoto Customer Support Center) for his great support for the measurement of ATR-FT-IR. This work was supported in parts by grants from Japan Science and Technology Agency (YS), the National Institutes of Health (Grants RO1HL39903 and HL079182 to M.S.) and the Department of Veterans Affairs Research Service (to M.S.).

Supporting Information Available: Details of compound syntheses. This material is available free of charge via the Internet at http://pubs.acs.org.

LITERATURE CITED

(1) Varki, A. (1999) In *Essentials of Glycobiology* (Varki, A., Cummings, R., Esko, J., Freeze, H., Hart, G., and Marth, J., Eds.), Cold Spring Harbor Laboratory Press, Cold Spring Harbor, New York, pp 57−68 and references therein.

(2) Gallagher, J. (2001) Heparan sulfate: growth control with a restricted sequence menu. *J. Clin. Invest. 108*, 357−361.

(3) Ostrovsky, O., Berman, B., Gallagher, J., Mulloy, B., Fernig, D. G., Delehedde, M., and Ron, D. (2001) Differential effects of heparin saccharides on the formation of specific fibroblast growth factor (FGF) and FGF receptor complexes. *J. Biol. Chem. 277*, 2444−2453.

(4) Faham, S., Hileman, R. E., Fromm, J. R., Linhardt, R. J., and Rees, D. C. (1996) Heparin structure and interactions with basic fibroblast growth factor. *Science 271*, 1116−1120.

(5) Horan, N., Yan, L., Isobe, H., Whitesides, G. M., and Kahne, D. (1999) Nonstatistical binding of a protein to clustered carbohydrates. *Proc. Natl. Acad. Sci. U.S.A. 96*, 11782−11786.

(6) Houseman, B. T., and Mrksich, M. (2002) Carbohydrate arrays for the evaluation of protein binding and enzymatic modification. *Chem. Biol. 9*, 443−454.

(7) Kato, M., and Mrksich, M. (2004) Using model substrates to study the dependence of focal adhesion formation on the affinity of integrin−ligand complexes. *Biochemistry 43*, 2699−2707.

(8) Fazio, F., Bryan, M. C., Blixt, O., Paulson, J. C., and Wong, C.-H. (2002) Synthesis of sugar arrays in microtiter plate. *J. Am. Chem. Soc. 124*, 14397−14402.

(9) Park, S., Lee, M.-R., Pyo, S.-J., and Shin, I. (2004) Carbohydrate chips for studying high-throughput carbohydrate-protein interactions. *J. Am. Chem. Soc. 126*, 4812−4819.

(10) Plant, A. L., Brigham-Burke, M., Petrella, E. C., and O'Shannessy, D. J. (1995) Phospholipid/alkanethiol bilayers for cell-surface receptor studies by surface plasmon resonance. *Anal. Biochem. 226*, 342−348.

(11) Peterlinz, K. A., and Georgiadis, R. (1996) In situ kinetics of self-assembly by surface plasmon resonance spectroscopy. *Langmuir 12*, 4731−4740.

(12) Liedberg, B., Nylander, C., and Lundström, I. (1983) Surface plasmon resonance for gas detection and biosensing. *Sens. Actuators 4*, 299−304.

(13) Flanagan, M. T., and Pantell, R. H. (1984) Surface plasmon resonance and immunosensors. *Electron. Lett. 20*, 968−970.

(14) Matsubara, K., Kawata, S., and Minami, S. (1988) Optical chemical sensor based on surface plasmon measurement. *Appl. Opt. 27*, 1160−1163.

(15) Suda, Y., Marques, D., Kermode, J. C., Kusumoto, S., and Sobel, M. (1993) Structural characterization of heparins binding domain for human platelets. *Thromb. Res. 69*, 501−508.

(16) Poletti, L. F., Bird, K. E., Marques, D., Harris, R. B., Suda, Y., and Sobel, M. (1997) Structural aspects of heparin responsible for interactions with von Willebrand factor. *Arterioscler., Thromb., Vasc. Biol. 17*, 925−931.

(17) Koshida, S., Suda, Y., Fukui, Y., Ormsby, J., Sobel, M., and Kusumoto, S. (1999) Synthesis of heparin partial structures and their binding activities to platelets. *Tetrahedron Lett. 40*, 5725−5728.

(18) Koshida, S., Suda, Y., Sobel, M., and Kusumoto, S. (2001) Synthesis of oligomeric assemblies of a platelet-binding key disaccharide in heparin and their biological activities. *Tetrahedron Lett. 42*, 1289−1292.

(19) Weis, C. D., and Newkome, G. R. (1990) Building-blocks for cascade polymers. 3. Facile elimination of nitrous-acid form quaternary nitroalkanes. *J. Org. Chem. 55*, 5801−5802.

(20) Ashton, P. R., Boyd, S. E., Brown, C. L., Nepogodiev, S. A., Meijer, E. W., Peerlings, H. W. I., and Stoddart, J. E. (1997) Synthesis of glycodendrimers by modification of poly(propylene imine) dendrimers. *Chem.—Eur. J. 3*, 974−984.

(21) Sobel, M., Soler, D. F., Kermode, J. C., and Harris, R. B. (1992) Localization and characterization of a heparin binding domain peptide of human von Willebrand factor. *J. Biol. Chem. 267*, 8857−886.

(22) Cruz, M. A., Handin, R. I., and Wise, R. J. (1993) The interaction of the von Willebrand factor A1 domain with platelet glycoprotein Ib Ix−The role of glycosylation and disulfide bonding in a monomeric recombinant A1 domain protein. *J. Biol. Chem. 268*, 21238−21245.

(23) Rastegar-Lari, G., Villoutreix, B. O., Ribba, A. S., Legendre, P., Meyer, D., and Baruch, D. (2002) Two clusters of charged residues located in the electropositive face of the von Willebrand factor A1 domain are essential for heparin binding. *Biochemistry 41*, 6668−6678.

(24) Presta, M., Maier, J. A., Rusnati, M., and Ragnotti, G. (1989) Basic fibroblast growth factor is released from endothelial extracellular matrix in a biologically active form. *J. Cell. Physiol. 140*, 68−74.

(25) Koshida, S., Suda, Y., Arano, A., Sobel, M., and Kusumoto, S. (2001) An efficient method for the assembly of sulfated oligosaccharides using reductive animation. *Tetrahedron Lett. 42*, 1293−1296.

(26) Ratner, D. M., Adams, E. W., Su, J., O'Keefe, B. R., Mrksich, M., and Seeberger, P. H. (2004) Probing protein−carbohydrate interactions with microarrays of synthetic oligosaccharides. *ChemBioChem 5*, 379−383.

(27) Suda, Y., Kusumoto, S., and Arano, A. (2003) Japan Patent P2003-83969A.

(28) Karamanska, R., Mukhopadyay, B., Russell, D. A., and Field, R.A. (2005) Thioctic acid amides: convenient tethers for achieving low nonspecific protein binding to carbohydrates presented on gold surfaces. *Chem. Commun.* 3334−3336.

(29) de Paz, J. L., Noti, C., and Seeberger, P. H. (2006) Microarrays of synthetic heparin oligosaccharides. *J. Am. Chem. Soc. 128*, 2766−2767.

(30) Feizi, T., and Chai, W. (2004) Oligosaccharide microarrays to decipher the glyco code. *Nat. Rev. 5*, 582−588.

BC0600620

Not Lipoteichoic Acid but Lipoproteins Appear to Be the Dominant Immunobiologically Active Compounds in *Staphylococcus aureus*[1]

Masahito Hashimoto,[2]* Kazuki Tawaratsumida,* Hiroyuki Kariya,* Ai Kiyohara,* Yasuo Suda,* Fumiko Krikae,† Teruo Kirikae,† and Friedrich Götz‡

Lipoteichoic acid (LTA) derived from *Staphylococcus aureus* is reported to be a ligand of TLR2. However, we previously demonstrated that LTA fraction prepared from bacterial cells contains lipoproteins, which activate cells via TLR2. In this study, we investigated the immunobiological activity of LTA fraction obtained from *S. aureus* wild-type strain, lipoprotein diacylglycerol transferase deletion (*Δlgt*) mutant, which lacks palmitate-labeled lipoproteins, and its complemented strain and evaluated the activity of LTA molecule. LTA fraction was prepared by butanol extraction of the bacteria followed by hydrophobic interaction chromatography. Although all LTA fractions activated cells through TLR2, the LTA from *Δlgt* mutant was 100-fold less potent than those of wild-type and complemented strains. However, no significant structural difference in LTA was observed in NMR spectra. Further, alanylation of LTA molecule showed no effect in immunobiological activity. These results showed that not LTA molecule but lipoproteins are dominant immunobiologically active TLR2 ligand in *S. aureus*. *The Journal of Immunology*, 2006, 177: 3162–3169.

Bacterial infection is one of the major causes of death. *Staphylococcus aureus*, a most common Gram-positive pathogen, is a major source of mortality in medical facilities (1). The pathogen causes various infectious diseases, including sepsis, endocarditis, and pneumonia. During the infection, *S. aureus* activates cells and evokes serious inflammation in the host. Lipoteichoic acid (LTA)[3] is a macroamphiphilic glycoconjugate distributing on the cell surface of Gram-positive bacteria and thought to be a virulence factor of Gram-positive bacteria (2). LTA are reported to exhibit immunostimulatory and inflammatory activities, including antitumor effect (3, 4), and induce inflammatory cytokines, such as TNF, IL-1, and IL-6 (5–7).

The innate immune system plays essential roles in host defense against bacterial infection. The system recognizes bacterial components known as pathogen-associated molecular patterns and controls immune responses. TLR, a type I transmembrane protein, has been found to be a major signaling receptor for pathogen-associated molecular patterns (8). To date, more than 10 members of the TLR family have been discovered and many ligands were identified. TLR4, the most characterized member of the family, in combination with an adapter molecule MD-2, has been shown to recognize LPS, an outer membrane component of Gram-negative bacteria (9, 10). TLR9 has been reported to be involved in immune responses to unmethylated CpG DNA (11) and TLR3 and TLR7/8 sense viral dsRNA and ssRNA (12, 13). Activation of TLR5 has been demonstrated to be mediated by bacterial flagellin (14). Bacterial lipoproteins have been found to be stimuli of TLR2 subfamily (TLR1, 2, and 6) (15, 16).

TLR2 has also been shown to play a crucial role in the host response to LTA fraction (17). Morath et al. (18, 19) also reported that LTA molecule from *S. aureus* was a potent stimulus of cytokine release. However, we have demonstrated that LTA from enterococci has no cytokine-producing activity. Fukase et al. (20, 21) prepared chemically synthetic glycoconjugates having fundamental structures of LTA from *Enterococcus hirae* and *Streptococcus pyogenes* and their glycolipid anchor parts, and Takada et al. (22) demonstrated that these synthetic compounds exhibited no immunostimulating activities. Furthermore, we found that a LTA fraction extracted from *E. hirae* can be separated into two subfractions, a small amount of cytokine-inducing active fractions and an inactive major compound, and the structure of the inactive compound is identical to that of LTA (23, 24). We also found that the enterococcal active fractions activate immune cells through TLR2 (25). These results suggest that the contaminating minor components in LTA fraction is responsible for the immunostimulant for TLR2.

We previously found that lipoproteins from *S. aureus* stimulate activation of immune cells through TLR2 (26). Furthermore, the activity of LTA fraction was decreased by lipoprotein lipase digestion, indicating that the fraction was contaminated by lipoproteins. Recently, Stoll et al. (27) constructed a lipoprotein diacylglycerol transferase (*lgt*) deletion mutant of *S. aureus*, which is unable to carry out lipid modification of prolipoproteins. It has been demonstrated that the mutant completely lacked palmitate-labeled lipoproteins and that the cells and crude lysate induced much less proinflammatory cytokines than the wild type (WT).

*Department of Nanostructure and Advanced Materials, Kagoshima University, Kagoshima, Japan; †Department of Infectious Diseases, International Medical Center of Japan, Tokyo, Japan; and ‡Mikrobielle Genetik, Universität Tübingen, Tübingen, Germany

Received for publication February 27, 2006. Accepted for publication June 19, 2006.

The costs of publication of this article were defrayed in part by the payment of page charges. This article must therefore be hereby marked *advertisement* in accordance with 18 U.S.C. Section 1734 solely to indicate this fact.

[1] This work was supported in part by Grants-in-Aid for Encouragement of Young Scientists (B) (16710160) from the Ministry of Education, Culture, Sports, Science and Technology and for Scientific Research (C) (17510179) from the Japanese Society of the Promotion of Science.

[2] Address correspondence and reprint requests to Dr. Masahito Hashimoto, Department of Nanostructure and Advanced Materials, Kagoshima University, Korimoto 1-21-40, Kagoshima 890-0065, Japan. E-mail address: hassy@eng.kagoshima-u.ac.jp.

[3] Abbreviations used in this paper: LTA, lipoteichoic acid; AB, alcian blue; BuOH, 1-butanol; HF, hydrofluoric acid; NMR, nuclear magnetic resonance; PEC, peritoneal exudate cell; PrOH, 1-propanol; TX-114, Triton X-114; WT, wild type.

0022-1767/06/$02.00

These results suggested that lipoproteins in *S. aureus* appear to be the predominant stimuli for the immune system. However, it is still unknown whether LTA molecule from *S. auerus* is inactive. In the present study, we prepared LTA fractions from the *S. aureus lgt* deletion mutant strain and analyzed its immunobiological activity and structure.

Materials and Methods

Bacterial culture and extraction of cell wall components

S. aureus SA113 WT, SA113 *lgt::ermB* (Δ*lgt*), and SA113 *lgt::ermB +pRBlgt* (+pRB) (27) organisms were grown in Mueller-Hinton II cation adjusted broth (BD Biosciences) at 37°C for 6 h with constant shaking. LTA factions of *S. aureus* were prepared by aqueous 1-butanol (BuOH) extraction method (19). Briefly, the cells were suspended in BuOH/water (1:1, v/v), and the mixture was stirred at room temperature for 30 min and centrifuged to separate aqueous phase from BuOH and cell debris. The aqueous phase was concentrated by evaporator, dialyzed for 3 days, and lyophilized to give crude LTA fraction. Crude fractions were further subjected to hydrophobic interaction chromatography on Octyl Sepharose 4FF (Amersham Biosciences). The fraction dissolved in 0.1 M ammonium acetate buffer (pH 4.7) containing 15% (v/v) 1-propanol (PrOH) was loaded to an Octyl Sepharose column (ϕ1.5 × 25 cm) equilibrated with the same buffer. The column was first eluted with 30 ml of equilibration buffer, with a linear PrOH gradient from 15 to 60% (v/v; 40 ml each), and then with 60% PrOH in the buffer. The fractions were collected every 3 ml (8 min) and analyzed by phosphorus content and NF-κB activation in Ba/mTLR2 cells described below. Bound fractions were combined, concentrated by evaporator, dialyzed, and lyophilized to give LTA fraction.

SA113 and SA113 *lgt::ermB* were also cultured in Brain heart infusion broth (BD Biosciences) adjusted to pH 6.0 with hydrochloric acid. LTA fractions were prepared by a similar method as above without dialysis steps. The fraction was again subjected to a column chromatography on Octyl Sepharose (ϕ1.5 × 20 cm) to separate a LTA and other active compounds. Hydrolysis of LTA molecules was performed with 47% aqueous hydrofluoric acid (HF) at 4°C for 24 h.

To extract a fraction containing lipoproteins, *S. aureus* cells were subjected to Triton X-114 (TX-114) phase partitioning, according to the method as reported (28). Briefly, the cells were suspended in PBS containing protease inhibitor mixture Complete mini (Roche Diagnostics) and combined with 1/10 volume of 10% aqueous TX-114. The mixture was rotated at 4°C for 1 h and then cell debris were centrifuged off. The supernatant was incubated and centrifuged at 37°C to separate TX-114 from aqueous phase. The upper aqueous phase was treated again with TX-114. Crude lipoprotein fraction was precipitated from TX-114 phase by addition of excess methanol.

Analytical methods

Phosphorous contents were measured by the method of Bartlett (29). SDS-PAGE was performed by the Tris-glycine method (30) using a mini PAGE chamber AE-6530 and an AE-8450 power supply (Atto Bioscience) with a 15% gel. Proteins were visualized by Coomassie brilliant blue staining and acidic materials, such as LTA, by alcian blue (AB) staining. Proton nuclear magnetic resonance (^{1}H NMR) spectra were measured using a ECA-600 spectrometer (JEOL) at 600 MHz at 293 K in D_2O. The chemical shifts are expressed in δ value with HOD (δ 4.67) as the internal standard.

Luciferase assays

Ba/F3 cells stably expressing p55IgκLuc, a NF-κB/DNA binding activity-dependent luciferase reporter construct (Ba/κB), murine TLR2 and the p55IgκLuc reporter construct (Ba/mTLR2), and murine TLR4/MD-2 and the p55IgκLuc reporter construct (Ba/mTLR4/mMD-2) were provided by Prof. K. Miyake (Institute of Medical Science, University of Tokyo, Tokyo, Japan). NF-κB-dependent luciferase activity in these cells was determined as described previously (31). Briefly, cells were inoculated onto each well of a 96-well flat-bottom plate (BD Biosciences) at 1×10^5 cells in 80 μl of RPMI 1640 (Sigma-Aldrich) supplemented with 10% FBS (MBL) and stimulated with the indicated concentrations of the test specimens. After 4 h of incubation at 37°C in humidified air containing 5% CO_2, 80 μl of Bright-Glo luciferase assay reagent (Promega) was added to each well, and luminescence was quantified with a luminometer ARVO SX multilabel counter (PerkinElmer). Results are shown as relative luciferase activity, which was the ratio of stimulated activity to nonstimulated activity, in each cell line.

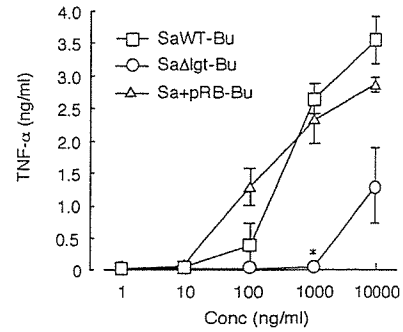

FIGURE 1. TNF-α production induced by the BuOH extracts of *S. aureus*, SaWT-Bu, Sa*Δlgt*-Bu, and Sa+pRB-Bu, in J774A.1 cells. J774A.1 were incubated with indicated concentrations of stimuli for 4 h. The levels of TNF-α in the culture supernatants were measured by ELISA. The data represent the mean and SD obtained from independent three experiments. *, Significantly different from the mean value of Sa*Δlgt*-Bu against SaWT-Bu (*, $p < 0.01$).

Cytokine assay

Eight-week-old male BALB/c and C57BL/6 mice were obtained from Kyudo. The animals received humane care in accordance with our institutional guidelines and the legal requirements of Japan. Elicited peritoneal macrophages were obtained from mice 3 days after i.p. inoculation of 1.0 ml of 3% sterile Brewer's thioglycolate broth (BD Biosciences). Peritoneal exudate cells (PEC) were centrifuged and suspended in RPMI 1640 supplemented with 10% FBS (Medical and Biological Laboratories). A mouse macrophage cell line, J774A.1 (Health Science Research Resource Bank), was cultured in DMEM (Sigma-Aldrich) supplemented with 10% FBS and

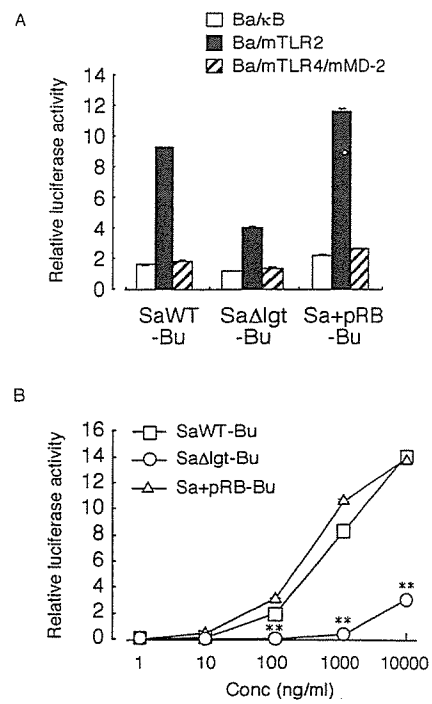

FIGURE 2. NF-κB activation in Ba/κB, Ba/mTLR2, or Ba/mTLR4/mMD-2 cells induced by SaWT-Bu, Sa*Δlgt*-Bu, and Sa+pRB-Bu. *A*, The cells were incubated with SaWT-Bu (1 μg/ml), Sa*Δlgt*-Bu (10 μg/ml), and Sa+pRB-Bu (1 μg/ml) for 4 h. *B*, The Ba/mTLR2 cells were incubated with indicated concentration of stimuli for 4 h. NF-κB activation was measured with a luciferase assay. Results are shown as relative luciferase activity, which was determined as the ratio of stimulated to nonstimulated activity. The data represent the mean and SD obtained from independent three experiments. *, Significantly different from the mean value of Sa*Δlgt*-Bu against SaWT-Bu (**, $p < 0.001$).

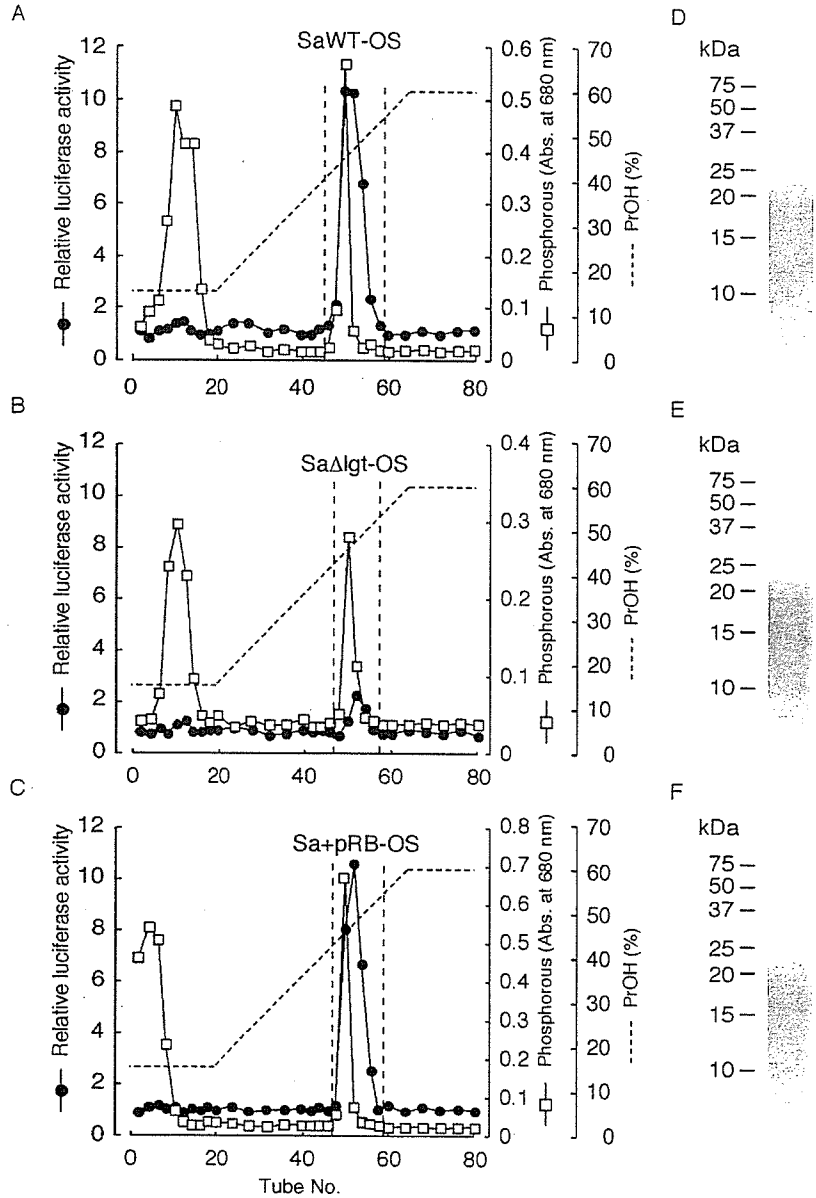

FIGURE 3. Separation of the BuOH extract by hydrophobic interaction chromatography on Octyl Sepharose 4FF. *A–C*, Elution profiles of the BuOH extracts, SaWT-Bu, SaΔ*lgt*-Bu, and Sa+pRB-Bu. The extract dissolved in 0.1 M ammonium acetate buffer (pH 4.7) containing 15% (v/v) PrOH was loaded to an Octyl Sepharose column (ϕ1.5 × 25 cm) equilibrated with the same buffer. The column was first eluted with 30 ml of equilibration buffer, with a linear PrOH gradient from 15 to 60% (v/v; 40 ml each) and then with 60% PrOH in the buffer. The fractions were collected every 3 ml (8 min) and analyzed by phosphorus content and NF-κB activation in Ba/mTLR2 cells. *D–F*, SDS-PAGE profiles of SaWT-OS, SaΔ*lgt*-OS, and Sa+pRB-OS. The fraction was separated by the Tris-glycine method with a 15% gel and visualized by AB.

also used for the assay. These cells were then distributed to 96-well plate at 2 × 10^5 cells/ml, after which they were incubated for 2 h at 37°C in humidified air containing 5% CO_2. Each dish was washed twice with PBS to remove nonadherent cells, and those attached to the dish served as peritoneal macrophages. Cells were stimulated with the indicated concentrations of the test specimens in culture medium supplemented with 10% FBS for 4 h at 37°C. After incubation, culture supernatants were collected and used for the cytokine assay using an ELISA kit for secreted TNF-α (R&D Systems). The concentration of secreted TNF-α from cells were determined using a standard curve of rTNF-α prepared in each assay. TNF-α concentrations in different experimental groups were analyzed for statistical significance by using Welch's *t* test.

Results

LTA fraction from S. aureus *SA113 Δlgt is less active than those from WT and the complemented strain*

It has been reported that *S. aureus* SA113 Δ*lgt* mutant and its crude cell lysate induce fewer proinflammatory cytokines and chemokines than its WT strain (27). Thus, the effect of the *lgt* deletion to immunostimulatory activity of LTA fraction was investigated. Crude LTA fractions were prepared by BuOH extraction, which was used for the LTA preparation by Morath et al. (18) from *S.*

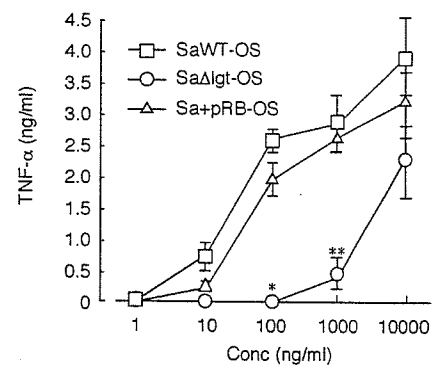

FIGURE 4. TNF-α production induced by the fractions eluted from Octyl Sepharose column, SaWT-OS, SaΔ*lgt*-OS, and Sa+pRB-OS, in J774A.1 cells. J774A.1 were incubated with indicated concentrations of stimuli for 4 h. The levels of TNF-α in the culture supernatants were measured by ELISA. The data represent the mean and SD obtained from independent three experiments. *, Significantly different from the mean value of SaΔ*lgt*-OS against SaWT-OS (*, $p < 0.01$; **, $p < 0.001$).

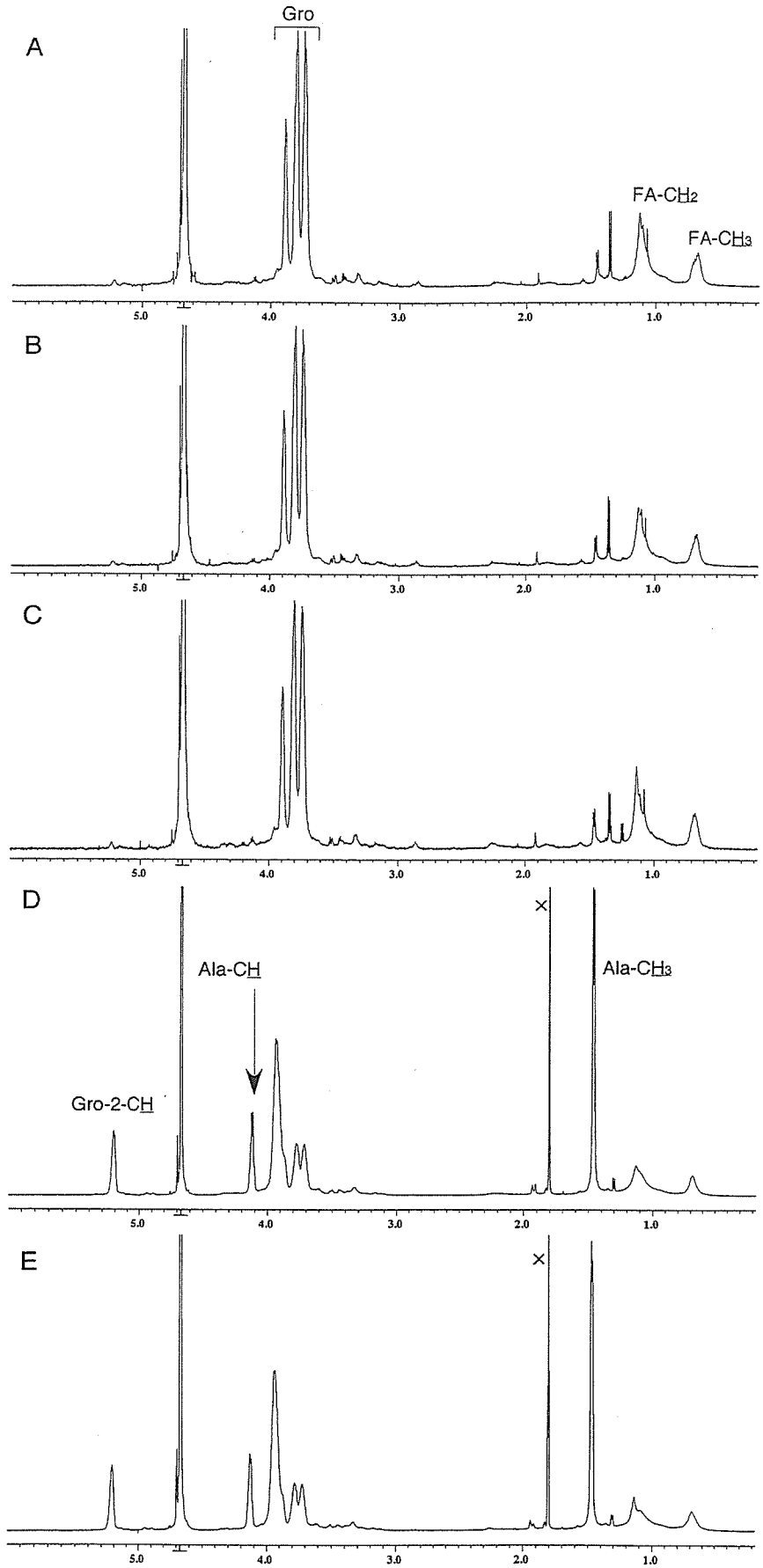

FIGURE 5. ^{1}H NMR spectra of the fractions. *A*, SaWT-OS. *B*, SaΔ*lgt*-OS. *C*, Sa+pRB-OS. *D*, SaWT6-OS. *E*, SaΔ*lgt*6-OS. Spectra were measured at 600 MHz at 293 K in D_2O. The chemical shifts are expressed in δ value with HOD (δ 4.67) as the internal standard.

aureus SA113 WT, Δ*lgt*, and +pRB strains. The yield of BuOH extracts were 0.8, 1.1, and 2.2% based on respective lyophilized cells and designated as SaWT-Bu, SaΔ*lgt*-Bu, and Sa+pRB-Bu, respectively. SaWT-Bu and Sa+pRB-Bu stimulated TNF-α production in J774A.1 at the concentration of 100 ng/ml (Fig. 1). In contrast, only slight TNF-α production was observed in J774A.1 stimulated with 10,000 ng/ml SaΔ*lgt*-Bu (Fig. 1), showing that the activity of SaΔ*lgt*-Bu is 100-fold lower than those of the others. All the BuOH extracts activated Ba/mTLR2 but not Ba/κB and Ba/mTLR4/mMD-2 (Fig. 2*A*), and the TLR2-mediated activity was dose dependent (Fig. 2*B*). These results suggested that TLR2 recognizes the extracts. The BuOH extracts were then subjected to hydrophobic interaction chromatography on Octyl Sepharose 4FF to separate LTA fraction from nucleic acids and cytoplasmic proteins. As shown in Fig. 3, *A–C*, LTA fraction was eluted at ca~40–50% PrOH concentration. The yield of LTA fraction were 6.5% (based on SaWT-Bu), 4.5% (based on SaΔ*lgt*-Bu), and 7.3% (based on Sa+pRB-Bu) and designated as SaWT-OS, SaΔ*lgt*-OS, and Sa+pRB-OS, respectively. SDS-PAGE profiles showed that all fraction contained AB-positive LTA (Fig. 3, *D–F*). SaWT-OS and Sa+pRB-OS stimulated TNF-α production in J774A.1 at the concentration of 10 ng/ml, whereas SaΔ*lgt*-OS stimulated TNF-α production only at concentrations > 1,000 ng/ml (Fig. 4), showing that the LTA fraction from Δ*lgt* deletion mutant is 100-fold less active than those from the others. These results suggested that lipoproteins are responsible for most of the activity of *S. aureus* LTA fractions.

Alanylation of LTA molecule showed no effect in the immunobiological activity

Morath et al. (18) reported that alanine substituent in LTA plays the critical role for the biological activity of LTA from *S. aureus*. Deliberate hydrolysis of alanine at pH 8.5 significantly reduced the activity of LTA. Thus, structures of the LTA fractions were analyzed by ^{1}H NMR to determined the alanine substitution. As shown in Fig. 5, *A–C*, no distinct difference was observed among the three LTA fractions. Methyl (δ 0.60–0.75) and methylene (δ 1.0–1.2) signals of fatty acids and methylene and methine (δ 3.7–3.9) of glycerol residues showed a *S. aureus*-type LTA structure. However, there is scarce signals of alanine attached to glycerol moieties, methyl (δ 1.45) and methine (δ 4.12), in alanine residue and methine (δ 5.22) of alanine-substituted glycerol, indicating the absence of alanine substitution in these LTA fractions. Previously, it has been shown that in *S. aureus* SA113 75% of the glycerol residues of LTA was esterified with D-alanine, whereas the corresponding *S. aureus dlt* mutant completely lacked LTA D-alanylation (32). The *dltABCD* operon encodes the genes for incorporation of D-alanine in teichoic acids. Furthermore, it is reported that the pH of culture medium affects the alanine ester content of LTA in *S. aureus* (33). LTA from organisms growing at high pH (pH 8.10) contained very little alanine ester, whereas high alanylation was observed at low pH (pH 6.07). Thus LTA fractions, named as SaWT6-OS and SaΔ*lgt6*-OS, were prepared by a similar method from *S. aureus* SA113 WT and Δ*lgt* strains grown at pH 6. In the NMR spectra, significant signals of alanines substituted at O2-position of glycerols in LTA was found in SaWT6-OS and SaΔ*lgt6*-OS (Fig. 5, *D* and *E*). SaWT6-OS, as well as SaWT-OS, stimulated TNF-α production in J774A.1, whereas the production by SaΔ*lgt6*-OS or SaΔ*lgt*-OS were 100- to 1000-fold less active (Fig. 6*A*). SaΔ*lgt*-OS or SaΔ*lgt6*-OS also induced less TNF-α production than the fractions from WT in murine PEC (Fig. 6, *B* and *C*). The activity of SaWT6-OS was comparable to SaWT-OS, and no significant enhancement was observed between SaΔ*lgt6*-OS and SaΔ*lgt*-OS. These results indicated that the alanylation of LTA molecule showed no significant effect on the immunobiological activity.

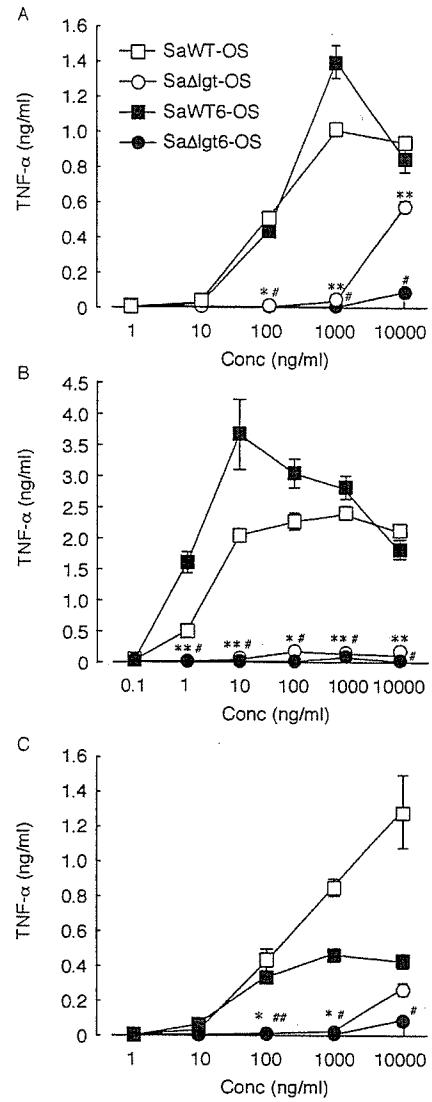

FIGURE 6. TNF-α production induced by the fractions eluted from Octyl Sepharose column, SaWT-OS, SaΔ*lgt*-OS, SaWT6-OS, and SaΔ*lgt6*-OS. *A*, J774A.1 were incubated with indicated concentrations of stimuli for 4 h. *B*, BALB/c PEC were incubated with indicated concentrations of stimuli for 4 h. *C*, C57BL/6 PEC were incubated with indicated concentrations of stimuli for 4 h. The levels of TNF-α in the culture supernatants were measured by ELISA. The data represent the mean and SD obtained from independent three experiments. *, Significantly different from the mean value of SaΔ*lgt*-OS against SaWT-OS (*, $p < 0.01$; **, $p < 0.001$). #, Significantly different from the mean value of SaΔ*lgt6*-OS against SaWT6-OS (#, $p < 0.01$; ##, $p < 0.001$).

TLR2-activating compounds in LTA fraction from Δlgt mutant are not LTA

SaΔ*lgt6*-OS still weakly activated Ba/TLR2 cells (data not shown), indicating that the fraction contained some TLR2-activating compound(s). Therefore, the fraction was again separated by hydrophobic interaction chromatography. The elution pattern of phosphate-rich LTA fraction was not the same as that of TLR2-active fraction (Fig. 7*A*). SaΔ*lgt6*-OS hydrolyzed with HF to cleave phosphodiester bonds in LTA molecules was also separated by the column. Hydrolyzed LTA fragments, phosphate, and derivatives of

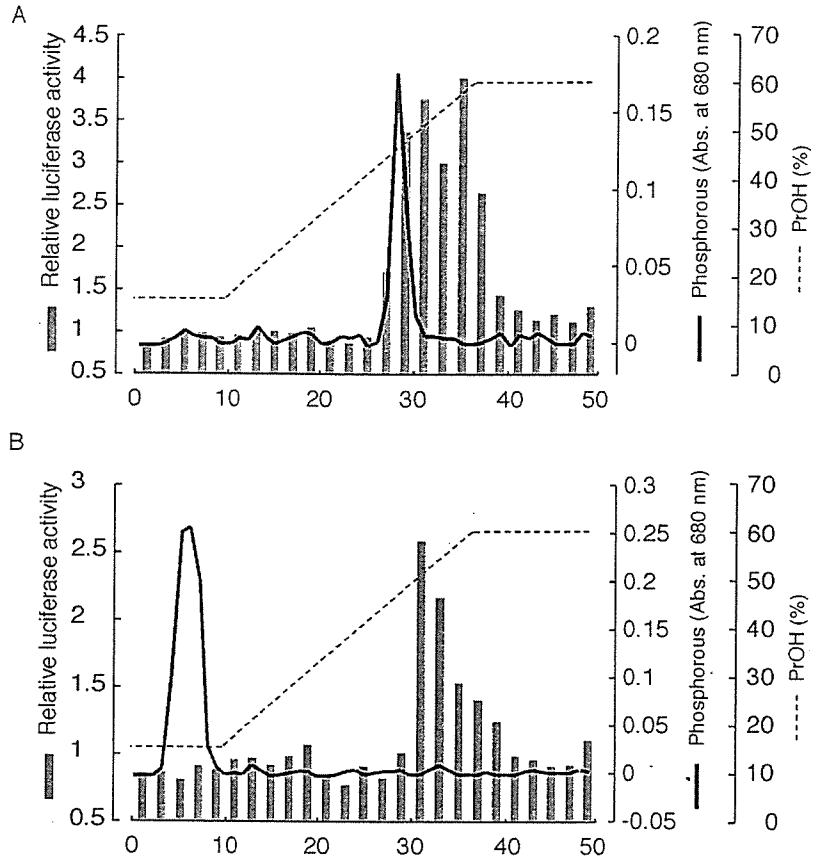

FIGURE 7. Separation of SaWT6-OS by hydrophobic interaction chromatography on Octyl Sepharose 4FF. *A*, Elution profiles of SaWT6-OS. *B*, Elution profiles of SaWT6-OS hydrolyzed with HF at 4°C for 24 h. The fraction dissolved in 0.1 M ammonium acetate buffer (pH 4.7) containing 15% (v/v) PrOH was loaded to an Octyl Sepharose column (ϕ1.5 × 20 cm) equilibrated with the same buffer. The column was first eluted with 30 ml of equilibration buffer, with a linear PrOH gradient from 15 to 60% (v/v; 40 ml each) and then with 60% PrOH in the buffer. The fractions were collected every 3 ml (8 min) and analyzed by phosphorus content and NF-κB activation in Ba/mTLR2 cells.

phosphoglycerol eluted as pass-through fraction, whereas TLR2-active fraction eluted at a similar PrOH concentration as that of SaΔ*lgt*6-OS (Fig. 7*B*). These results suggested that the fraction contains unknown TLR2-activating compound other than LTA molecule.

Discussion

We previously demonstrated that lipoprotein fraction extracted from *S. aureus* WT using TX-114 phase partitioning activate immune cells via TLR2 (26). The lipoprotein lipase digestion of the fraction abrogated its activity, suggesting that lipoproteins is a potent TLR2 ligand in *S. aureus*. Recently, Stoll et al. (27) constructed a *lgt* deletion mutant of *S. aureus*, which completely lacked palmitate-labeled lipoproteins, and found it immunobiologically less active than WT. These results indicated that the predominant TLR2-activating components in *S. aureus* are lipoproteins. LTA is thought to be a potent immunostimulating component in Gram-positive bacteria. However, we have shown that highly purified LTA from *E. hirae* is inactive, but minor contaminants are active (23, 24). In the present study, we confirmed that the LTA fraction from Δ*lgt* mutant, SaΔ*lgt*-OS, is 100-fold less potent than those of WT, SaWT-OS (Figs. 1 and 4). These observations clearly show that most of the activity of LTA fraction obtained from natural sources is attributable to the lipoproteins contaminated in the fraction. We recently demonstrated that a mAb, mAbEh1, established by immunization of the active subfraction of *E. hirae* LTA fraction, neutralized the activity not only of LTA fraction from *E. hirae* and *S. aureus* but also immunobiologically active bacterial lipopeptides, Pam_3CSK_4 and FSL-1 (M. Hashimoto, submitted for publication). These results strongly support the above consideration. Some LPS preparations have been shown to slightly induce a signal via TLR2, in addition to TLR4 (34, 35). The activity is proven to be the result of lipoprotein contamination in these preparations (31, 36). LPS is an amphiphile, which consists of hydrophobic glycolipid moiety and hydrophilic polysaccharide, and considered to work as a detergent to coextract lipoproteins from bacterial cells in a LPS extraction step. Since LTA is also an amphiphile, LTA may play a similar role as LPS.

For many decades, it has been controversial as to whether the LTA molecule exhibits immunostimulating activities. Recently, Morath et al. (18) suggested that partial degradation of LTA during the separation steps contributed to the activity. In our previous experiments, inactive LTA was prepared by the phenol-hot water extraction method (23, 24), whereas Morath et al. (18) obtained LTA by amended BuOH-water extraction and found that D-alanine contents in phenol-extracted LTA is less than those in BuOH one. They also showed that alkaline hydrolysis of the active LTA, which resulted in a loss of D-alanine substituent in LTA, reduced its activity. Thus, they concluded that D-alanine content in a LTA molecule is critical for the activity of LTA from *S. aureus*. However, we demonstrated here that D-alanine content has no significant effect on the activity of LTA fraction. We compared the levels of alanine substitution in LTA obtained from *S. aureus* grown in the different conditions. All LTA fractions cultured in neutral pH scarcely contained alanine substituent (Fig. 5, *A–C*). However, SaWT-OS and Sa+pRB-OS exhibited potent immunostimulating activities (Fig. 4), whereas both LTA fractions from pH 6 medium contained considerable alanine substituent (Fig. 5, *D* and *E*). Despite alanine substitution, SaΔ*lgt*6-OS exhibited significantly low activity compared with SaWT6-OS (Fig. 6). In the fraction from WT strain, SaWT-OS and SaWT6-OS, the LTA alanylation showed no significant effects on TNF-α production (Fig. 6). These

results prove that not the D-alanine content but the lipoprotein contaminant is responsible for the activities of LTA fractions. The alanylation may affect some of LTA properties, but the activity of the fraction is independent of alanylation. The previous observation may be artificial due to the process of alkaline hydrolysis.

Immunologically inactive LTA has not been obtained from *S. aureus*. We have previously purified inactive LTA from *E. hirae* using hydrophobic interaction, followed by anion exchange chromatography (23). Morath et al. (18) purified *S. aureus* LTA by a similar method and found that cytokine-inducing activity coeluted with phosphate derived from LTA. Therefore, they concluded that LTA is a potent stimuli for cytokine release in immune cells and that a contamination by other bacterial components in the *S. aureus* LTA is unlikely. We were also unable to isolate a completely inactive LTA from *S. aureus* even if using Δ*lgt* mutant (Fig. 3). However, the precise elution of SaΔ*lgt*6-OS on Octyl Sepharose column showed that TLR2 activity eluted broadly, but most of the activity was separated from a sharp LTA-derived phosphate peak (Fig. 7*A*). Furthermore, the active compound eluted at similar fractions after HF degradation of LTA (Fig. 7*B*). HF hydrolyzed phosphodiester linkages in LTA and cleaved into hydrophilic inorganic phosphate and derivatives of phosphoglycerol and hydrophobic diacylglycerol-type glycolipid; the former was shown to be inactive (Fig. 7*B*), and the latter was also demonstrated to be inactive at least in our assay system using chemically synthetic compound (M. Hashimoto, submitted for publication). The activity of the contaminant after LTA degradation seems to be diminished (Fig. 7*B*) compared with that before degradation (Fig. 7*A*). It may be caused by loss of solubilization capacity of LTA. These results suggest that fraction contains some TLR2-activating contaminants, but it is independent of LTA molecule.

The minor active contaminants in the LTA fraction of Δ*lgt* mutant are still unidentified. The TLR2-activating compound was also extracted by TX-114 phase partitioning of the mutant (data not shown). TX-114 is usually used for extraction of hydrophobic compounds. The chromatographic property and extraction behavior suggested that the compounds may be acylated. Recently, Uehori et al. (37) reported that monoacylated muramyldipeptide derivatives, which mimic peptidoglycan structure of bacillus Calmette-Guerin, activated DC through TLR2/TLR4. Since unmodified muramyldipeptide did not activate cells via TLR but through NOD2 (38), specific acylation might be required for TLR activation. Furthermore, the contaminants activated J774A.1 and PEC from C57BL/6 but not PEC from BALB/c (Fig. 6). A distinct set of gene expression may be required for cells activation. It is possible that small amount of hydrophobic acylated compounds are present in the LTA fraction.

In conclusion, we demonstrated here that LTA fraction obtained from *S. aureus* Δ*lgt* mutant is 100-fold less potent than those of WT, and the activity is independent from extraction methods of the fraction and D-alanine contents in LTA molecule. Lipoproteins but not LTA molecule are the predominant TLR2-activating components in *S. aureus*.

Acknowledgments

We thank Professor Kazuhisa Sugimura at Kagoshima University for measuring luciferase activities.

Disclosures

The authors have no financial conflict of interest.

References

1. Lowy, F. D. 1998. *Staphylococcus aureus* infections. *N. Engl. J. Med.* 339: 520–532.
2. Fischer, W. 1990. Bacterial phosphoglycolipids and lipoteichoic acid. In *Glycolipids, Phosphoglycolipids and Sulfoglycolipids*, M. Kates, ed. Plenum Press, New York, pp. 123–234.
3. Yamamoto, A., H. Usami, M. Nagamuta, Y. Sugawara, S. Hamada, T. Yamamoto, K. Kato, S. Kokeguchi, and S. Kotani. 1985. The use of lipoteichoic acid (LTA) from *Streptococcus pyogenes* to induce a serum factor causing tumour necrosis. *Br. J. Cancer* 51: 739–742.
4. Usami, H., A. Yamamoto, W. Yamashita, Y. Sugawara, S. Hamada, T. Yamamoto, K. Kato, S. Kokeguchi, H. Ohokuni, and S. Kotani. 1988. Anti-tumour effects of streptococcal lipoteichoic acids on Meth A fibrosarcoma. *Br. J. Cancer* 57: 70–73.
5. Usami, H., A. Yamamoto, Y. Sugawara, S. Hamada, T. Yamamoto, K. Kato, S. Kokeguchi, H. Takada, and S. Kotani. 1987. A nontoxic tumour necrosis factor induced by streptococcal lipoteichoic acids. *Br. J. Cancer* 56: 797–799.
6. Tsutsui, O., S. Kokeguchi, T. Matsumura, and K. Kato. 1991. Relationship of the chemical structure and immunobiological activities of lipoteichoic acid from *Streptococcus faecalis* (*Enterococcus hirae*) ATCC 9790. *FEMS Microbiol. Immunol.* 3: 211–218.
7. Bhakdi, S., T. Klonisch, P. Nuber, and W. Fischer. 1991. Stimulation of monokine production by lipoteichoic acids. *Infect. Immun.* 59: 4614–4620.
8. Underhill, D. M., and A. Ozinsky. 2002. Toll-like receptors: key mediators of microbe detection. *Curr. Opin. Immunol.* 14: 103–110.
9. Poltorak, A., X. He, I. Smirnova, M. Y. Liu, C. Van Huffel, X. Du, D. Birdwell, E. Alejos, M. Silva, C. Galanos, et al. 1998. Defective LPS signaling in C3H/HeJ and C57BL/10ScCr mice: mutations in *Tlr4* gene. *Science* 282: 2085–2088.
10. Shimazu, R., S. Akashi, H. Ogata, Y. Nagai, K. Fukudome, K. Miyake, and M. Kimoto. 1999. MD-2, a molecule that confers lipopolysaccharide responsiveness on Toll-like receptor 4. *J. Exp. Med.* 189: 1777–1782.
11. Hemmi, H., O. Takeuchi, T. Kawai, T. Kaisho, S. Sato, H. Sanjo, M. Matsumoto, K. Hoshino, H. Wagner, K. Takeda, and S. Akira. 2000. A Toll-like receptor recognizes bacterial DNA. *Nature* 408: 740–745.
12. Alexopoulou, L., A. C. Holt, R. Medzhitov, and R. A. Flavell. 2001. Recognition of double-stranded RNA and activation of NF-κB by Toll-like receptor 3. *Nature* 413: 732–738.
13. Heil, F., H. Hemmi, H. Hochrein, F. Ampenberger, C. Kirschning, S. Akira, G. Lipford, H. Wagner, and S. Bauer. 2004. Species-specific recognition of single-stranded RNA via Toll-like receptor 7 and 8. *Science* 303: 1526–1529.
14. Hayashi, F., K. D. Smith, A. Ozinsky, T. R. Hawn, E. C. Yi, D. R. Goodlett, J. K. Eng, S. Akira, D. M. Underhill, and A. Aderem. 2001. The innate immune response to bacterial flagellin is mediated by Toll-like receptor 5. *Nature* 410: 1099–1103.
15. Takeuchi, O., T. Kawai, P. F. Muhlradt, M. Morr, J. D. Radolf, A. Zychlinsky, K. Takeda, and S. Akira. 2001. Discrimination of bacterial lipoproteins by Toll-like receptor 6. *Int. Immunol.* 13: 933–940.
16. Takeuchi, O., S. Sato, T. Horiuchi, K. Hoshino, K. Takeda, Z. Dong, R. L. Modlin, and S. Akira. 2002. Cutting edge: role of Toll-like receptor 1 in mediating immune response to microbial lipoproteins. *J. Immunol.* 169: 10–14.
17. Schwandner, R., R. Dziarski, H. Wesche, M. Rothe, and C. J. Kirschning. 1999. Peptidoglycan- and lipoteichoic acid-induced cell activation is mediated by Toll-like receptor 2. *J. Biol. Chem.* 274: 17406–17409.
18. Morath, S., A. Geyer, and T. Hartung. 2001. Structure-function relationship of cytokine induction by lipoteichoic acid from *Staphylococcus aureus*. *J. Exp. Med.* 193: 393–397.
19. Morath, S., A. Stadelmaier, A. Geyer, R. R. Schmidt, and T. Hartung. 2002. Synthetic lipoteichoic acid from *Staphylococcus aureus* is a potent stimulus of cytokine release. *J. Exp. Med.* 195: 1635–1640.
20. Fukase, K., T. Matsumoto, N. Ito, T. Toshimura, S. Kotani, and S. Kusumito. 1992. Synthetic study on lipoteichoic acid of Gram positive bacteria. I. Synthesis of proposed fundamental structure of *Streptococcus pyogenes* lipoteichoic acid. *Bull. Chem. Soc. Jpn.* 65: 2643–2654.
21. Fukase, K., T. Toshimura, S. Kotani, and S. Kusumito. 1994. Synthetic study of lipoteichoic acid of Gram positive bacteria. II. Synthesis of the proposed fundamental structure of *Enterococcus hirae* lipoteichoic acid. *Bull. Chem. Soc. Jpn.* 67: 473–482.
22. Takada, H., Y. Kawabata, R. Arakaki, S. Kusumoto, K. Fukase, Y. Suda, T. Yoshimura, S. Kokeguchi, K. Kato, T. Komuro, et al. 1995. Molecular and structural requirements of a lipoteichoic acid from *Enterococcus hirae* ATCC 9790 for cytokine-inducing, antitumor, and antigenic activities. *Infect. Immun.* 63: 57–65.
23. Suda, Y., H. Tochio, K. Kawano, H. Takada, T. Yoshida, S. Kotani, and S. Kusumoto. 1995. Cytokine-inducing glycolipids in the lipoteichoic acid fraction from *Enterococcus hirae* ATCC 9790. *FEMS Immunol. Med. Microbiol.* 12: 97–112.
24. Hashimoto, M., J. Yasuoka, Y. Suda, H. Takada, T. Yoshida, S. Kotani, and S. Kusumoto. 1997. Structural feature of the major but not cytokine-inducing molecular species of lipoteichoic acid. *J. Biochem.* 121: 779–786.
25. Hashimoto, M., Y. Imamura, T. Morichika, K. Arimoto, O. Takeuchi, K. Takeda, S. Akira, K. Aoyama, T. Tamura, S. Kotani, et al. 2000. Cytokine-inducing macromolecular glycolipids from *Enterococcus hirae*: improved method for separation and analysis of its effects on cellular activation. *Biochem. Biophys. Res. Commun.* 273: 164–169.
26. Hashimoto, M., K. Tawaratsumida, H. Kariya, K. Aoyama, T. Tamura, and Y. Suda. 2006. Lipoprotein is a predominant Toll-like receptor-2 ligand in *Staphylococcus aureus* cell wall components. *Int. Immunol.* 18: 355–362.

27. Stoll, H., J. Dengjel, C. Nerz, and F. Götz. 2005. *Staphylococcus aureus* deficient in lipidation of prelipoproteins is attenuated in growth and immune activation. *Infect. Immun.* 73: 2411–2423.
28. Shibata, K., A. Hasebe, T. Sasaki, and T. Watanabe. 1997. *Mycoplasma salivarium* induces interleukin-6 and interleukin-8 in human gingival fibroblasts. *FEMS Immunol. Med. Microbiol.* 19: 275–283.
29. Bartlett, G. R. 1959. Phosphorus assay in column chromatography. *J. Biol. Chem.* 234: 466–468.
30. Laemmli, U. K. 1970. Cleavage of structural proteins during the assembly of the head of bacteriophage T4. *Nature* 227: 680–685.
31. Hashimoto, M., Y. Asai, and T. Ogawa. 2004. Separation and structural analysis of lipoprotein in a lipopolysaccharide preparation from *Porphyromonas gingivalis*. *Int. Immunol.* 16: 1431–1437.
32. Peschel, A., M. Otto, R. W. Jack, H. Kalbacher, G. Jung, and F. Götz. 1999. Inactivation of the dlt operon in *Staphylococcus aureus* confers sensitivity to defensins, protegrins, and other antimicrobial peptides. *J. Biol. Chem.* 274: 8405–8410.
33. MacArthur, A. E., and A. R. Archibald. 1984. Effect of culture pH on the D-alanine ester content of lipoteichoic acid in *Staphylococcus aureus*. *J. Bacteriol.* 160: 792–793.
34. Kirschning, C. J., H. Wesche, T. Merrill Ayres, and M. Rothe. 1998. Human Toll-like receptor 2 confers responsiveness to bacterial lipopolysaccharide. *J. Exp. Med.* 188: 2091–2097.
35. Kirikae, T., T. Nitta, F. Kirikae, Y. Suda, S. Kusumoto, N. Qureshi, and M. Nakano. 1999. Lipopolysaccharides (LPS) of oral black-pigmented bacteria induce tumor necrosis factor production by LPS-refractory C3H/HeJ macrophages in a way different from that of Salmonella LPS. *Infect. Immun.* 67: 1736–1742.
36. Lee, H. K., J. Lee, and P. S. Tobias. 2002. Two lipoproteins extracted from *Escherichia coli* K-12 LCD25 lipopolysaccharide are the major components responsible for Toll-like receptor 2-mediated signaling. *J. Immunol.* 168: 4012–4017.
37. Uehori, J., K. Fukase, T. Akazawa, S. Uematsu, S. Akira, K. Funami, M. Shingai, M. Matsumoto, I. Azuma, K. Toyoshima, et al. 2005. Dendritic cell maturation induced by muramyl dipeptide (MDP) derivatives: monoacylated MDP confers TLR2/TLR4 activation. *J. Immunol.* 174: 7096–7103.
38. Inohara, N., Y. Ogura, A. Fontalba, O. Gutierrez, F. Pons, J. Crespo, K. Fukase, S. Inamura, S. Kusumoto, M. Hashimoto, et al. 2003. Host recognition of bacterial muramyl dipeptide mediated through NOD2: implications for Crohn's disease. *J. Biol. Chem.* 278: 5509–5512.

ヘパリンと血小板ならびにフォンビルブラント因子との相互作用解析からシュガーチップの開発へ

隅田泰生
鹿児島大学大学院理工学研究科
ナノ構造先端材料工学専攻

[Summary]
Heparin, used clinically as an anticoagulant, is a highly sulfated natural polysaccharide and is composed of various distinct partial structures. Recently, heparin has drawn more attention, since it possesses regulatory functions for cell proliferation, through the direct binding interaction with growth factors. We have studied heparin-platelet and heparin-von Willbrand factor interactions using a synthetic approach with structurally defined heparin partial structures. Through this work, we found that the assembly of the structurally defined oligosaccharides was needed to mimic nature, and we also lacked sufficient mass of oligosaccharides to study their function at the molecular level. To resolve both issues, we have developed a novel, molecular level technology – the oligosaccharide-immobilized chip (named Sugar Chip). This permits real-time and high-throughput analysis of oligosaccharide-protein interactions without any labeling of the targeted protein, using these Sugar Chips and the surface plasmon resonance (SPR) apparatus.

キーワード：ヘパリン、構造特異性、オリゴ糖鎖、部分構造、結合相互作用、無標識、チップ、表面プラズモン共鳴、血小板、フォンビルブラント因子、糖鎖結合性蛋白質

1. ヘパリンと血小板ならびにフォンビルブラント因子との相互作用解析

1．1　ヘパリンについて

抗血液凝固剤として知られるヘパリンは、高濃度に硫酸化されている天然多糖であり、抗血液凝固活性以外にも近年では細胞増殖の調製因子としての活性が注目されている[1-5]。ヘパリンの構造的特徴は、一言でいえば不均一、即ち非常に多くの部分構造の混合物であるということである。たとえば、図1にはヘパリンの部分構造の1つを示している。この中の右から3つ目からの五糖構造は、抗血液凝固活性を担う最小単位であるAntithrombin IIIとの結合ドメインとして同定されたもの[6,7]である。五糖には3単位のグルコサミンと2単位のウロン酸があるが、全て構造が異なっている糖分子から構成されている。

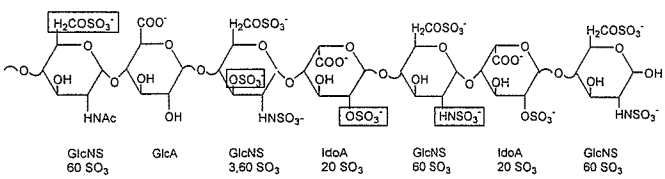

図1　ヘパリンの構造の不均一性

1．2　ヘパリンと血小板相互作用

1．2．1　構造推定

ヘパリンは抗血液凝固剤であり、第2次大戦頃から臨床の場において使用されているが、1970年頃からヘパリンによって血小板が凝集するという現象論が報告されていた[8]。筆者は、この現象を分子レベルで解析する研究を、1988年頃からDr. Sobel（現在、米国ワシントン大学医学部）とともに行った。前述したように、ヘパリンの構造は単純ではなく、また血小板のどの蛋白質がこの現象に関係しているかという情報もなかった。そこで、まずヘパリンを既知の3つの方法で低分子化した後、分子量と電荷によって分画し、一連の低分子化ヘパリン（LMWH）を調製し、それらの活性を測定することによって、血小板に結合するヘパリンの部分構造を推定しようとした[9]。3つの方法は、図2に示すが、亜硝酸での分解、過ヨウ素酸でvic-diolの酸化と引き続くb脱離反応による分解、酵素（ヘパリナーゼI）による酵素消化である。

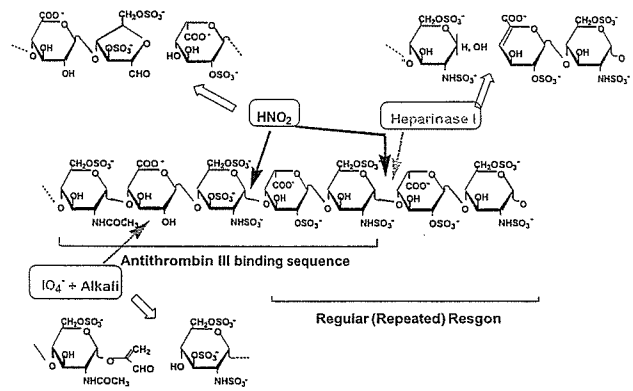

図2　ヘパリンの分解とドメイン構造の例

ラジオアイソトープ標識したヘパリンの血小板への結合を、調製したLMWHがどれくらい強く阻害するかを調べるBinding Competition Assayを行った。実験を迅速に行うためにラジオアイソトープとして^{125}ヨウ素を用いたが、そのために混合するだけでヘパリンの水酸基と共有結合できる新規修飾試薬も開発した[10]。それぞれの阻害活性を各々のLMWHの血小板への結合能として評価し、図3に示した。横軸はLMWHの平均分子量、縦軸は血小板への結合能である。いずれも分子量が大きいほど結合活性が高く

なっているが、色分けしている様に、ヘパリンの低分子化の方法によって傾向が異なることがわかった。即ち、ヘパリナーゼで低分子化したLMWH(HI-Hep)と亜硝酸分解のLMWH(NA-Hep)はほぼ同じ集合の中にあるが、過ヨウ素酸とアルカリで分解して調製したLMWH(PI-Hep)はそれらより上にプロットされた。即ちより強い活性を持つ集合を形成していることがわかった。一方、これらLMWHの抗血液凝固活性は抗第10因子活性（anti-Xa活性、antithrombin IIIとヘパリンの活性をもっとも直接的に見ることができる）を調べてみると、図中に数字（大きいほど活性が高い）を示したように、PI-Hepの活性はほとんどないことがわかった。

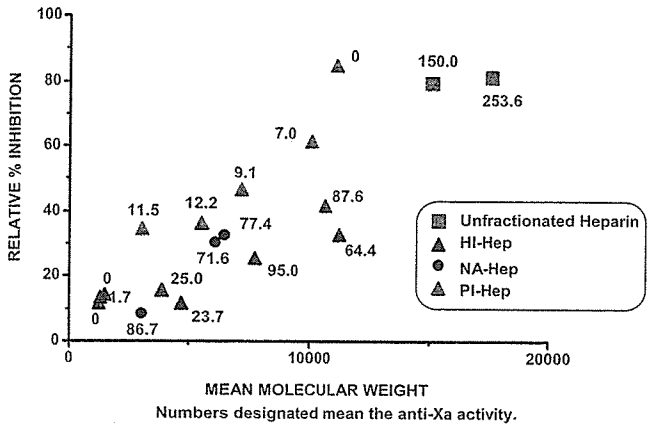

図3　低分子化ヘパリン（LMWH）の血小板結合活性

低分子化反応によって消失する構造を考える（図2参照）と、PI-HepではAntithrombin IIIに結合する五糖構造の中にvic-diol構造があり、これが過ヨウ素酸で酸化して環が開裂し、引き続くアルカリ処理でβ脱離がおこるので、五糖構造が消失する。それ故、PI-Hepはanti-Xa活性が激減すると考えられるが、結果はその通りになっていた。一方、血小板結合能はanti-Xa活性ほどはっきりしていないが、分子量11000程度のLMWHを比較してみると、PI-Hepは分画していないヘパリンと変わらない活性を持っているが、Hi-Hepは半分以下の活性となっている。即ち、ヘパリナーゼ処理によって消失した構造が血小板結合に重要な役割を持っていると考え、図中のGlcNS6S-IdoA2Sと略した二糖構造を血小板結合最小構造と推定した。

1．2．2　合成化合物による推定構造の確定

推定した二糖構造がはたして本当に血小板結合性があるのか、これを確定させるためにこの二糖構造を合成することにした[11]。図4に合成ルートを示したが、硫酸化オリゴ糖の合成は初めてだったので、大学院生と試行錯誤しながら進め、1年以上がかかったが、SynDSと命名した二糖を10数ミリグラム得た。

この合成硫酸化二糖(SynDS)の活性を、同様の結合阻害実験を行い調べた。陽性コントロールとしてはヘパリン、二糖の比較対照としてはヘパリンをヘパリナーゼで徹底的に消化して得られる二糖構造（図中DigDSと略）を用いた。DigDSはSynDSと同じ数の硫酸基、カルボキシル基を持つ二糖であるが、構造は全く

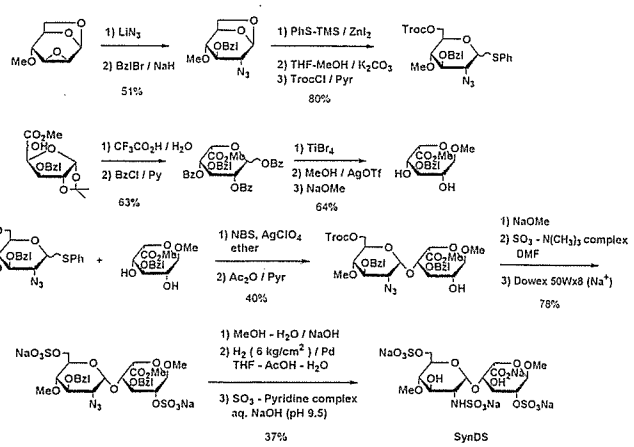

図4　GlcNS6S-IdoA2S構造を有するヘパリン部分二糖構造の合成

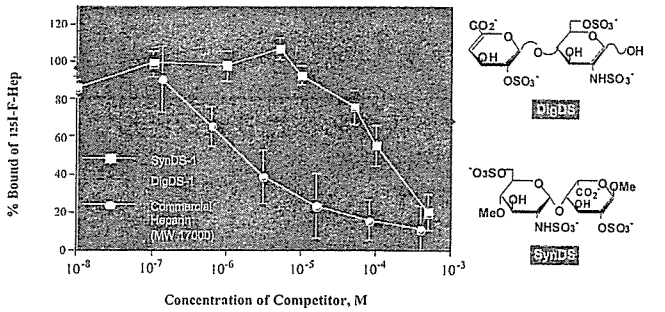

図5　合成ヘパリン部分二糖構造の血小板結合挙動

異なる。SynDSは、陽性コントロールのヘパリンと比べると活性は弱く、かなりの高濃度を必要とするが、DigDSと比べると明確に活性があることが示された。これから、ヘパリン中のヘパリナーゼ消化で消失する二糖構造GlcNS6S-IdoA2Sを血小板結合に関する最小構造と結論した。

1．2．3　集合化化合物の合成と血小板結合活性

ところで図3のように、活性はLMWHの分子量に依存していた。このことは、最小二糖構造に基づくクラスター効果の影響であると考え、次に複数のGlcNS6S-IdoA2Sユニットを有する構造明確な合成化合物を得ることを目指した。

この際、硫酸化糖であることから、工夫が必要になった。即ち、一般的な方法では、まず保護基を有する糖鎖前駆体を調製し、それを集合化した後、脱保護、硫酸化を行う。しかし、実際やってみると二糖構造が3単位ある化合物までは、何とか合成することができたが[12]、4単位以上では硫酸基がすべて入らず、不均一な化合物ができてしまった。そこで、二糖では硫酸基をすべて導入できていることから発想を変えて、ユニットの硫酸化二糖構造を完成させたのち、マイルドな反応によって、ユニットごと集合させる方法を考えた（図6参照）。